Genetic diversification in the Tropical Western Atlantic Ocean

Phylogeography of the gastropod *Bulla occidentalis*

Thesis for the degree of Master of Science in Biology

Biodiversity, evolution and ecology

by Jørgen Aarø

Department of Biology

University of Bergen

June 2011

TABLE OF CONTENTS

1. ABSTRACT

The region under study is the Tropical Western Atlantic (TWA) which includes the Caribbean Sea with adjacent coastlines, the Gulf of Mexico, Bermuda and the coast of South America down to the tropical/temperate transitional zone near Uruguay. There are several examples of genetic breaks within the Caribbean that have been attributed to oceanographic factors, transient allopatry, as well as ecological factors, but no common biogeographical pattern has been found and mechanisms behind diversification within the region are not fully understood. The aim of this project was to shed light on diversification patterns of shallow-water soft-bottom invertebrates in the TWA by using the gastropod *Bulla occidentalis* as a model species. The following questions were adressed: (1) Is *B. occidentalis* a homogenous genetic entity or is it made-up of more than one genetic partition (ESUs) as hypothesized by Malaquias and Reid (2009)? (2) What caused the pattern of genetic discontinuities (ESUs)? (3) Are the genetic breaks shared with other species? and (4) Are there periods of major expansion or contraction in population size and what may have caused these events? Material was obtained from museum collections and through fieldwork, and sequences fragments of the cytochrome *c* oxidase subunit I (COI) and 16S rRNA mitochondrial genes were amplified and sequenced using standard methods. Population genetic indices such as number of haplotypes, haplotype diversity, nucleotide diversity, and fixation indices were estimated, and statistical parsimony haplotype networks for the individual genes were constructed to assess the population structure. The *B. occidentalis* species genealogy with divergence times between main lineages was estimated based on calibration with the oldest known fossil attributed to the *B. occidentalis* lineage (Early Miocene, 20,43 – 15,97 Mya) under the assumption of a strict molecular clock. Isolation-by-distance methods were employed to test correlation between genetic differentiation and geographic distance. The demographic history was reconstructed using a Bayesian Skyline method. The *B. occidentalis* population showed a structured genealogy with three ESUs (A: all coastline samples from Brazil to Eastern Florida, including Yucatan and the islands of Guadeloupe and Bermuda; B: all samples from the Florida Keys; C: predominantly Cuban samples). The three lineages had an average genetic distance of 4,6% – 5,9% (uncorrected *p*-distance). Divergence between the three lineages was dated to the Late Miocene (11,06 – 6,11 Mya), and may have been caused by vicariance related to the Panamanian Isthmus up-lift. The mechanisms maintaining divergence of these lineages are difficult to pinpoint because no direct link was established between the geographical subdivision and present oceanographic patterns, ecological factors or Isolation-by-distance. Genetic divergence of the Florida Keys-lineage mirrors

patterns found in other groups. The genealogy and demographic history reconstruction showed an increase in genetic diversification and effective population size during the Pleistocene. This coincides with an increase in the magnitude of glaciation cycles that may have caused periods of transient allopatry likely reducing population connectivity leading to genetic diversification, as well as potentially creating new niche-opportunities during low sea-level stands allowing the population to expand.

2. INTRODUCTION

2.1. Biogeography of the Tropical Western Atlantic

The aim of phylogeography is to understand intra-specific and species-complex patterns of divergence and how they coincide with present-day and historical geologic and geographic features and processes (Chan *et al.* 2011). The geographical area under study in this research project is the Tropical Western Atlantic (TWA) as defined by Spalding *et al.* (2007): the Caribbean Sea with adjacent coastlines, Bermuda and the coast of South America down to the tropical/temperate transitional zone near Uruguay, but in addition including the Gulf of Mexico.

The TWA is a region that has been through large changes in recent geological history. The rise of the Panamanian Isthmus, a process taking place over 12 million years, and reaching completion approximately 2.8 Ma ago, had large consequences for ocean circulation patterns, global climate, and evolution of both marine and terrestrial organisms (Coates and Obando 1996; Lessios 2008). The changes in the Tropical Western Atlantic environment included new current patterns as well as raised temperature and salinity, which in turn marked the onset of glaciaction cycles and increasing eustatic changes during the Pliocene (5,332-2,588 Mya) and Pleistocene periods (2,588 Mya – 12 Kya) (Lessios 2008).

The TWA is traditionally divided into distinct biogeographic provinces identified and characterized by unique assemblages of species and clades, but the exact names, numbers and boundaries of these provinces vary somewhat between authors (summarized by Reid (2009)). At least two provinces are commonly recognized within the TWA, the Caribbean and the Brazilian (Reid 2009), but a separate West Indian province (including Bermuda, the Bahamas, the Leeward and Windward Antilles Islands) has also been suggested (Briggs 1974). The northern bound of the Caribbean province is placed somewhere along the east coast of the United States in a transition zone between Warm-Temperate and Tropical climates and another such transitional zone was placed on the gulf-side of the Florida peninsula, based on many examples of faunal breaks between Tropical Florida and the temperate Gulf of Mexico (Briggs 1974). North of the Caribbean province lies the Carolinian, and the division between these two have a long history dating back to the Early Miocene, represented by the Caloosahatchian province (North Carolina to Florida and the Yucatán peninsula) and the Gatunian province (includes the Caribbean) (Vermeij 2005). A major feature along the north-eastern

coast of South America, separating the Caribbean and Brazilian provinces is the Amazon Barrier, which is created by freshwater run-off from the Orinoco and Amazon rivers that was established in its present form during the Pliocene (Briggs 1974; Campbell Jr. e*t al.* 2006)). This over 2300 kilometre stretch of coastline is influenced by sediment-rich freshwater forming a plume of lower salinity that represents a biogeographic barrier for many species (Rocha 2003). The Brazilian province stretches to the southern transitional zone between tropical and warm-temperate climates near Uruguay.

Taxonomically based biogeographic subdivisions have traditionally been defined by unique assemblies of groups at low taxonomic levels. These are, however, seldom exhaustive. For instance the system proposed by Briggs (1974) was mostly based on fish, and for the Caribbean, subdivision has largely been based on taxonomic levels in the range from Class to Family (Miloslavich *et al.* 2010). Recently an attempt was made at making a global classification of the marine environment based on the presence of homogenous composition of species, and the predominance of a small number of ecosystems, oceanographic and topographic features (Spalding *et al.* 2007), but this was not consistently supported by a later regionalization (Miloslavich *et al.* 2010). Focus on certain taxonomic groups or focusing on higher taxonomic levels will result in species distributions sometimes failing to be consistent with established subdivisions (Miloslavich *et al.* 2010). For bivalves and gastropods in the Caribbean no general pattern of species distributions exists (with exceptions in Yucatán and Belize), suggesting that distribution of species in the Caribbean is controlled by availability of different habitat types (Miloslavich *et al.* 2010). There are, however, certain examples of groups at low taxonomic levels (genus and family) that show specific patterns in their distribution due to vicariant events during the evolution of the Caribbean Sea, and this variation can be masked if focus lies on higher taxonomic levels (Miloslavich *et al.* 2010). Miloslavich *et al.* (2010) suggest that the Caribbean as a whole is a distinctive sub-region of the Northern Tropical Western Atlantic Province, but that the region is not biogeographically uniform due to its complex geological history, and present-day geographic variation in hydrologic and habitat regimes.

2.2. Genetic discontinuities in the Tropical Western Atlantic

A large part of the TWA is the Caribbean Sea, which is known to be a marine biodiversity hotspot (Roberts *et al.* 2002; Miloslavich *et al.* 2010) despite being a fairly compact area with few obvious

physical barriers and large degree of faunal homogeneity (Taylor and Hellberg 2006; Reid 2009). Despite this perceived uniformity there are several examples of established genetic breaks within species, suggesting that some drivers of genetic differentiation do exist (*Brachidontes exustus,* Lee and Ó Foighil 2005; *Elacatinus sp.,* Taylor and Hellberg 2006; *Bulla occidentalis,* Malaquias and Reid 2009; *Cittarium pica,* Diaz-Ferguson *et al.* 2010). Both ecological and vicariant explanations have been offered, but the processes seem to differ between different animal groups, and patterns of genetic discontinuities do not seem consistent between animal groups (Taylor and Hellberg 2006; Rocha *et al.* 2008; Diaz-Ferguson *et al.* 2010).

Strong evidence was found for the presence of a phylogenetic break in the Mona Passage between the islands of Hispaniola and Puerto Rico islands for different ecologies of the coral reef fish genus *Elacatinus* (Taylor and Hellberg 2006). The strong northbound current through the passage was thought to inhibit dispersal between the two islands, thereby causing a genetic discontinuity. Weak support for a genetic barrier was also found in the Exuma Sound of the Bahamas, but if present, this is likely established later than the Mona barrier (Taylor and Hellberg 2006).

Another approach for identifying genetic discontinuities and recognizing regions of high connectivity, thereby also biogeographic break points, is by the use of hydrodynamic models of larval dispersal (fish, Cowen *et al.* 2006). Cowen *et al.* (2006) detected the presence of four such connectivity-regions, corresponding to the Eastern Caribbean, Western Caribbean, the Bahamas-region and the coastlines influenced by the Colombia-Panama gyre. The central Caribbean was suggested to be a zone of admixture, mediating a low level of connectivity between regions. These four connectivity regions were only partly supported by the genetic structure of the trochid gastropod *Cittarium pica* (Diaz-Ferguson *et al.* 2010). A low level of differentiation was uncovered between the Eastern Caribbean and the Bahamas, a Venezuelan population that was expected to group with the Eastern Caribbean proved to be differentiated from all other groups and a Panamanian population was strongly differentiated from geographically close populations in Panama and Costa Rica. The authors viewed their results as supporting the Carribean as a uniform biogeographical province, with high genetic diversity due to meso-scale oceanographic features (Diaz-Ferguson *et al.* 2010). For instance, the Colombia-Panama gyre is likely causing some isolation in the area encompassed by the coastlines of Colombia, Panama, Costa Rica and Nicaragua, as is evident from the mentioned modelling experiment (Cowen *et al.* 2006) and from the trochid gastropod *Cittarium pica* (Diaz-Ferguson *et al.* 2010). The Antilles Current (Figure 1) is

weak compared to the other mentioned currents which potentially creates a difference in dispersal capacity in a East-North direction compared to a East-West direction along the Caribbean current. Figure 2 depicts variation in coastline range with variable sea levels, which likely made an impact of connectivity within the adjacent areas of the Caribbean sea. This possibility is especially relevant when discussing Pleistocene glacial cycles that have been taking place in the last 2,5 million years (Lessios 2008; Miller *et al.* 2005). There is evidence for periods (or pulses) with a high rate of mollusc extinctions and species origination in the Pleistocene, and these glaciation events could be directly related to the diversification of Western Atlantic shallow water organisms (Lessios 2008). Transient allopatry has been suggested as a potential mechanism producing species pairs along single coastlines in the TWA and in the Tropical East Pacific Ocean for example in calyptraid gastropods (Collin 2003).

2.3. Physical and geological description of the Tropical Western Atlantic Ocean

The flow of surface currents can have implications for potential genetic connectivity in marine populations (White *et al.* 2010), and an understanding of the ocean surface current system in the TWA is therefore a vital piece of the puzzle in uncovering underlying causes for genetic discontinuities. The online service Ocean Surface Currents summarizes data from a vast amount of literature on ocean surface currents. For convenience we divide the review into two parts; the Caribbean Sea (including Tropical Florida) with the Gulf of Mexico, and the outer-Atlantic region (Bermuda, Brazil, and the Atlantic ocean east of the Antilles). The most relevant and general information is included here to produce a broad picture of the Tropical Western Atlantic surface current-system, but for detailed information on the current system, see the Ocean Surface Currents website (http://oceancurrents.rsmas.miami.edu/index.html).

2.3.1. The outer-Atlantic region

The South Equatorial Current system is a mainly westward-bound current system that is found in the Central Tropical Atlantic ocean and is deflected into northbound and southbound currents where it hits the easternmost region on the Brazilian mainland near 14ºS (Bonhoure *et al.* 2004). Water from the South Equatorial Current system that is deflected to the north feeds the North Brazil Current, which travels along the Brazilian Bahia State at an average speed of around 60-100 cm/s until it reaches the coast of Guyana. A part of the water from the South Equatorial Current system

travels in a north-eastward direction, feeding the North Equatorial Counter-Current or feeding the Caribbean Current depending on the season (Bischof *et al.* 2003). The North Brazil Current feeds the Guiana Current which has a mean velocity that is measured to be 41.6 cm/s. The Guiana Current enters the Caribbean Sea mostly through the Windward Islands and constitutes the majority of the water that enters the Caribbean Sea (about 70%). The Guiana Current varies in flow velocity during the year, and with the peak speeds observed in April-May and a minimum speed in September. The Antilles Current flows from the northern Lesser Antilles north-west into the Florida Current, but is of a variable nature and its existence has been discussed (Rowe *et al.* 2011).

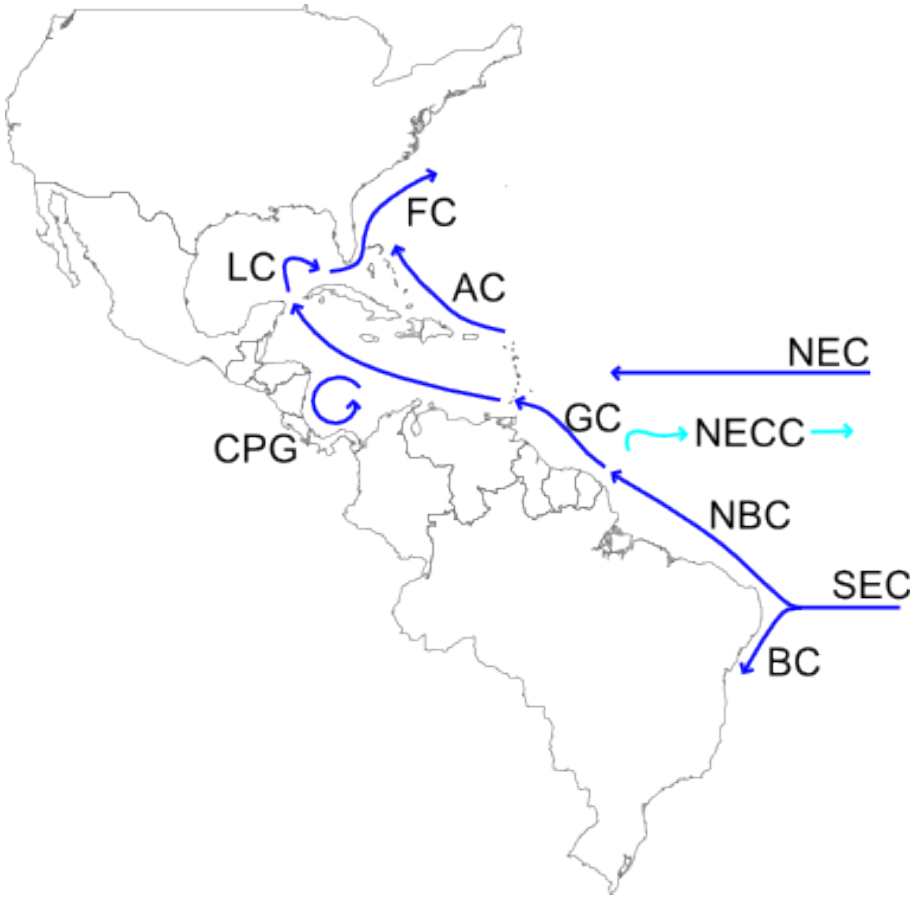

Figure 1: Overview of the Tropical Western Atlantic Ocean current system.

Table 1: Estimates of surface current travel distances and velocities
(Data gathered from http://oceancurrents.rsmas.miami.edu/ and Google Earth)

Current name	Ca. dist. (km)	V (cm/s)	V (km/day)	Distance travelled per n days (km)		
				10	14	21
CC (Aves ridge to Florida strait) Low		30	26	259	363	544
CC High	2800	40	35	346	484	726
AC (British Virgin Islands – Northern Bahamas) H		9	8	78	109	163
AC Low	1800	4	3	35	48	73
GC (Guiana-Antilles)	1300	42	36	359	503	755
NBC (Bahia tip-Guiana) High		100	86	864	1210	1814
NBC Low	2221	60	52	518	726	1089

2.3.2. The Caribbean Sea and the Gulf of Mexico

The majority of sampling localities in this project are located in or adjacent to the Caribbean sea, which is a semi-enclosed basin in the Western Atlantic Ocean surrounded by the Atlantic-side coastlines of Northern-, Middle and South America and the Lesser Antilles Island Arc. The main circulation direction in the Caribbean Sea is counter-clockwise, with water entering in the south-west through the Lesser Antilles arc and exiting in the north-west between Florida and Cuba becoming the beginning of the Gulf Stream that flows along the east coast of Florida and into the Northern Atlantic. Deep water does not enter the Caribbean Sea because of the shallow depths in the Lesser Antilles Arc, and the upper 1200 meters of the water body of the Caribbean is stratified with little deep-water circulation (Gyory *et al.* [2011a]). The sea bottom topography of the Caribbean Sea can be divided into five basins separated by underwater ridges (Miloslavich *et al.* 2010), a feature that has implication for creating meso-scale eddies in Caribbean surface-currents (Andrade and Barton 2000). The depths of these basins are abyssal with over half of the Caribbean Sea deeper than 3600 meters, and an average depth of 2200 meters (Isaza *et al.* 2006; Miloslavich *et al.* 2010) while the ridges and plateaus separating are shallower, for instance the Gorda Bank off the coast of Honduras which in some areas is less than 20 meters deep. The Caribbean Current is fed by the Guiana Current mainly through the Grenada, St. Vincent and St. Lucia passages in the Windward Island group (Gyory *et al.* [2011a]). The Caribbean Current has a general flow in an east-west direction in the Caribbean Sea from the Lesser Antilles to the Yucatan Strait, with the strongest flow in the southernmost third of the Caribbean Sea, velocity reaching 70 cm/s. The current system in the Caribbean Sea does show both seasonal and spatial variation, but the exact nature of this variability is not fully resolved (see Gyory *et al.* [2011a] for discussion). Both meso-scale meanders and eddies have been detected, as well as larger gyre systems. A clockwise-circulating gyre (the Colombia-Panama Gyre) has been suggested to exist off the coast of Panama, but the exact nature of this is at this point elusive (Gyory *et al.* [2011a]).

Water from the Caribbean Sea enters into the Gulf of Mexico through the straits of Yucatan that separates Cuba from the Yucatan peninsula. This flow feeds the current system in the Gulf of Mexico, the most important in this context being the Loop Current. This current is the flow that feeds both the Yucatan Current and the eastward-flowing Florida Current that exits the Caribbean Sea between Cuba and Florida. The position of the Loop Current is interchanging, variably feeding the Florida Current and the Yucatan Current. The Florida Current is fed by the Loop Current and the

Antilles Current with the main portion coming from the Loop Current, which is considered to be the beginning of the Gulf Stream (Gyory *et al.* [2011b]).

2.3.3. Bathtmetry and sea level variation

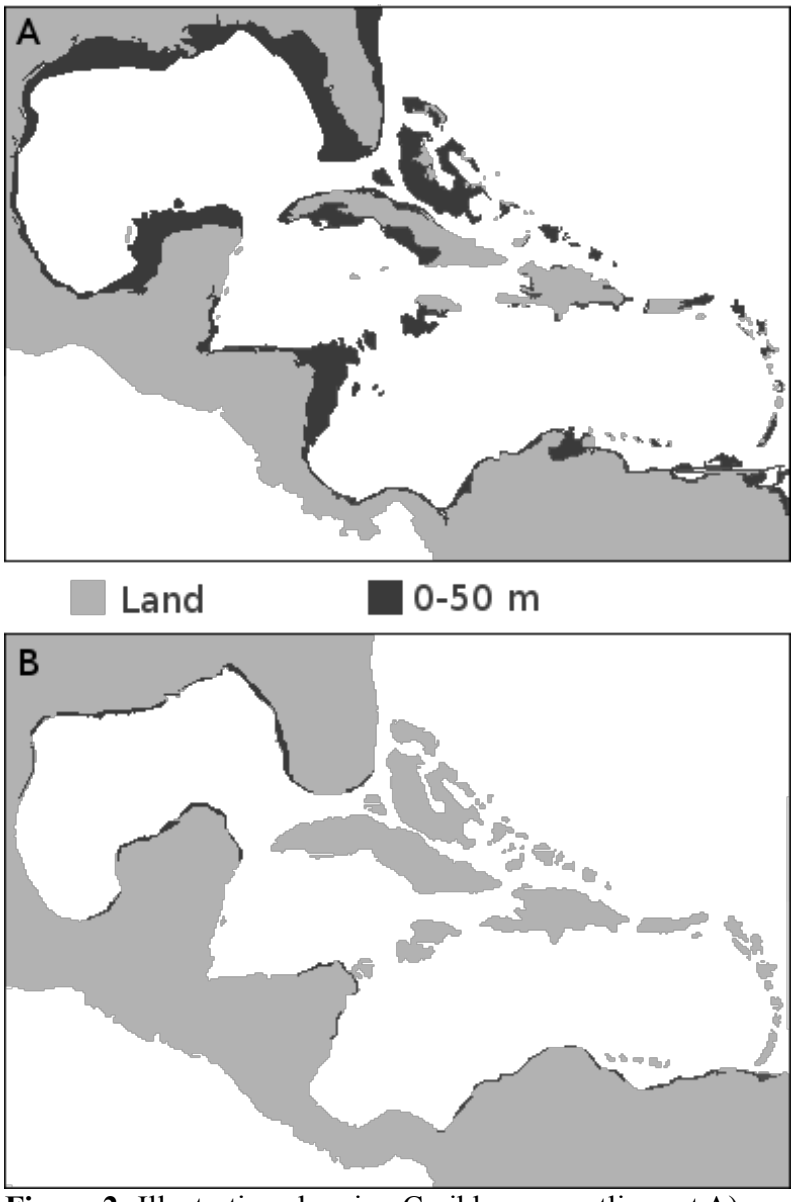

Figure 2: Illustration showing Caribbean coastlines at A) present sea level B) Sea-level 150 meters below todays level (as during Pleistocene glacial maxima). Dark grey areas show depths of 0-50 m. Adapted from Bellwood and Wainwright (2002).

Global sea level changes (eustasy) related to the formation and melting of continental ice-sheets can happen very rapidly, up to 200 meters pr. thousand years for the formation of ice-sheets and

resulting sea-level drop, and 20 meters related to melting and resulting sea-level rise (Miller *et al.* 2005). Global sea-level changes from the Oligocene to the Early Pliocene were in the order of around 30 to 60 meters, relating mainly to the behaviour of the Antarctic ice-sheet (Miller *et al.* 2005). Formation and decay of large ice-sheets in the northern hemisphere with correspondingly large sea-level changes have taken place during the last 2,5 million years, from the late Pliocene to the present, initiated by climatic effects of the closing of the Panamanian Isthmus (Miller *et al.* 2005). In the Northern Atlantic a relationship between complex evolutionary histories and global glaciation cycles have been detected in *Littorina* as a consequence of changes in the availability of suitable habitat due to eustatic changes (Doellman *et al.* 2011). The effect of glaciation cycles on tropical benthic soft-bottom communities inhabiting oceanic islands is poorly understood (Cuhna *et al.* 2011). During periods of low sea-level stands in the Pliocene and Pleistocene the implications for species inhabiting soft-bottom and hard-bottom substrates on oceanic islands in the Pacific ocean were different with soft-bottom species experiencing local extinctions due to habitat loss and hard-bottom communities showed elevated speciation rates due to new niche opportunities (Paulay 1990).

With the Plio-Pleistocene low sea-level stands causing sea levels to drop around 100-150 meters (Miller *et al.* 2005; Haq, Hardenbol and Vail (1988) in Cunha *et al.* 2011), both habitat loss and population connectivity in the TWA could have been affected in severe ways. Figure 2 shows the 50 m isobaths (underwater sea-bottom contour line at a specific depth) with today's sea-water level, and with a global sea-level 150 meters below present levels. With a sea-level drop of 150 meters, the reduction in continental shelf-area would be 89%, potentially decreasing the availability of estuaries, lagoons and other shallow-water habitat types (Bellwood and Wainwright 2002).

2.4. Model species: *Bulla occidentalis*

2.4.1. Phylogeny, ecology and palaeontological history

Bulla occidentalis (Figure 3) is one of twelve species in the genus *Bulla*, the only genus in the family Bullidae of cephalaspidean opistobranch gastropods. Two *Bulla* species exist in the TWA, *B. occidentalis* and *B. solida,* but the sister species of *B. occidentlais* is *B. striata* (Malaquias and Reid 2008). *B. striata* is found in the Eastern Atlantic Ocean and the Mediterranean Sea (Malaquias and Reid 2008). The species-pair is not possible to distinguish morphologically, but do show reciprocal

monophyly for the COI, 16S and 28S genes is are for this reason recognized as different species (Malaquias and Reid 2008, 2009). This clade appears marginally earlier in the fossil record in the Eastern Atlantic (Aquitainian, 23–20 Ma) compared with the Western Atlantic (Burdigalian, 20–16 Ma) and has an estimated divergence time of 20.4 – 27.3 Mya (Malaquias and Reid 2008, 2009). This led Malaquias and Reid (2008, 2009) to suggest a westward direction of trans-Atlantic dispersal for this clade.

B. occidentalis is found in shallow waters with sandy or muddy bottom down to about 3 meter depths, typically in estuaries or lagoons (Malaquias and Reid 2009). They are herbivores feeding on green algae and benthic phytoplankton. *B. occidentlais* have slender shells with thick shell walls and an involute spire, and an approximate maximum length of 45 mm. The colour of the shell varies between different brownish tones. The animal itself is brown with bright white dots (Figure 3). Colour tones of the shell and animal body can vary between localities. *B. occidentalis* is distributed throughout the TWA, from southern Brazil near the tropical/warm-temperate transitional zone in Uruguay in the south, throughout the Caribbean Sea and in the Gulf of Mexico and northwards to Bermuda (Malaquias and Reid 2008).

Figure 3: Live specimen of *Bulla occidentalis*. Photo: Manuel A. E. Malaquias.

B. occidentalis are hermaphroditic with sexual reproduction involving copulation with internal fertilization. They are seasonal spawners with a one-year life-cycle, and have been reported as common in November in Brazil (Malaquias and Reid 2008), and specimens were found abundantly

in Venezuela during March 2010 (M. A. E. Malaquias), Panama during June 2010 (M. Kambestad), and Guadeloupe in July 2010 (by the author). In the latter three cases the specimens were not yet full adults. They produce an egg-mass that is deposited on benthic vegetation, often sea-grass (Malaquias and Reid 2008). Little is known about the dispersal capabilities of *B. occidentalis,* as these have never been specifically studied. The precence of a planktotrophic veliger larva has been detected in *B. gouldiana*, *B. solida* and *B. striata*, but the exact longevity is not known. Larval development of *B. striata* has been observed under experimental conditions, and shown to last at least ten days (Murillo and Templado 1998). However, in this study the development was prematurely terminated so this can only serve as a minimum estimate of larval longevity. The detected presence of a planktotrophic veliger larva in three different *Bulla* species and similarities between the protoconch of all *Bulla* could be an indication for similar development throughout the genus (Malaquias and Reid 2009). Typically, shelled cephalspids with indirect development last in average two to four weeks in the plankton (Schaeffer 1996).

2.4.2. Genetic differentiation

B. occidentalis is considered to be a single species, but harbours a large degree of genetic differentiation within its distributional range. Malaquias and Reid (2009) identified four Evolutionary Significant Units (ESUs) with genetic distance between 5,5% - 8% (uncorrected *p*-distance for the COI mitochondrial gene). The explanation for this large genetic differentiation was suggested to be related to ecological selection across continental and oceanic lineages (Malaquias and Reid 2009). The differences in habitats are thought to be due to larger nutrient influx to the continental shelf by freshwater run-off from the continents as well as upwelling, while oceanic environments like in the Caribbean islands are thought to be poorer in nutrients. This explanation has been suggested for different organisms (*Brachidontes exustus,* Lee and Ó Foighil 2005; *Bulla occidentalis,* Malaquias and Reid 2008; *Echinolittorina,* Reid 2009). Because of a small sample size (n=20), the result could only be seen as provisional, and the need for further examination was suggested by the authors. An increase in samples size and sampling localities will give the analysis better resolution to discover patterns at a more detailed level, as well as lowering the influence of sampling stochasitcity in the observed pattern.

2.5. Choice of genetic markers

The mitochondrial COI-gene was selected as an appropriate marker for this study because of its potential to reveal intra-specific genetic variability. Because mitochondrial DNA has a smaller effective population size (N_e) than nuclear DNA, variation in the mitochondrial genome becomes detectable at a more rapid pace (Sunnucks 2000). The less variable mitochondrial 16S rRNA gene was also selected for use as a marker. COI is a protein-coding gene while 16S is a structural rRNA subunit in the mitochondrial ribosome and both are part of the same locus, but are under different selective pressures due to functional constraints (Mueller 2006). Previous work on *B. occidentalis* used both COI and 16S as genetic markers (Malaquias and Reid 2008, 2009), making it practical to continue using these two as this data could be easily included in this study. In addition, COI and 16S are commonly used markers in phylogeographic studies of marine invertebrates (*Siphonaria pectinata,* gastropod, Kawauchi and Giribet 2001; *Patelloida profunda,* gastropod, Kirkendale and Meyer 2004; *Doris kerguelenensis,* nudibranch, Wilson *et al.* 2009; *Brachidontes puniceus,* mussel, Cuhna *et al.* 2011).

2.6. Project aims

This phylogeographic study aims to contribute to the increased understanding of diversification of shallow-water benthic organisms inhabiting soft-bottom habitats in the Western Tropical Atlantic Ocean. This will be accomplished by further investigating the observed genetic diversity and phylogeographic discontinuities detected in *Bulla occidentalis* by Malaquias and Reid (2009), which in this context serves as a model organism. The data-set used by the latter authors will be expanded both in number of specimens and localities, and Bayesian phylogenetic inference calibrated with fossil data will be use to establish the genealogy and the time of diversification events. The demographic history of the species will be inferred by Bayesian Skyline reconstruction, and standard population genetic methods will be applied to uncover patterns of population structure. The outcomes from these analyses will be related to past and present ecological, geological, and oceanographic conditions in the TWA in an effort to uncover patterns and potential causes of marine diversification in *B. occidentalis*. This will hopefully contribute to increasing the general understanding of marine biogeography and diversification patterns in the Western Tropical Atlantic Ocean.

We aim to answer the following questions:

1) Is *Bulla occidentalis* a homogenous genetic entity or is it made-up of more than one genetic partition (ESUs) as hypothesized by Malaquias and Reid (2009)?
2) What caused the pattern of genetic discontinuities (ESUs)?
    - Isolation due to geographical distance between localities?
    - Isolation due to ecological selection: segregation across oceanic versus insular habitats?
    - Current Ocean circulation patterns and surface current-mediated genetic connectivity?
    - Pliocene-Pleistocene eustatic changes?
    - Vicariant events in the geological evolution of the Tropical Western Atlantic Ocean?
3) Are the genetic breaks shared with other species?
4) Are there periods of major expansion or contraction in population size and what may have caused these events?

3. MATERIAL AND METHODS

3.1. Sampling

Specimens were acquired from museum collections as well as through field work performed by the candidate, main supervisor, student colleagues and other acquaintances. A total number of 84 new specimens have been used for DNA-extraction to produce a total dataset of 98 sequences including sequences downloaded from GenBank (see Figure 4 for sampling sites, Table 2 for sample list and Appendix I for detailed information). Field-work was performed by snorkelling and the collection itself was done by hand picking or by use of simple tools like kitchen sieves. Collected specimens were immediately preserved in 96% ethanol with ethanol volume approximately 3 times larger than the volume of specimens in jars.

Table 2: Sample locations, coordinates, number of samples pr. locality and pr country (localities including sequences from GenBank marked with *)

Country	Location	Coordinates (approx)	No. of samples	Total no. of samples
Bermuda	Tom Moore's pond	32.20 N – 64.42 W	8	8
East Florida	St. Lucie inlet *	27.10 N – 80.08 W	14	14
Florida Keys	Pigeon Key *	24.42 N – 81.09 W	1	6
	Long Key *	24.49 N – 80.49 W	2	
	Pine Channel *	24.41 N – 81.23 W	3	
Cuba (south)	Guanahacabibes *	21.51 N – 84.38 W	1	13
	Cabo de San Antonio *	21.51 N – 84.57 W	4	
	Playa Giron	22.03 N – 81.02 W	6	
	Bahia de Cienfuegos	22.05 N – 80.23 W	2	
Mexico	Laguna de Chelem	21.15 N – 89.44 W	8	8
Panama	Bocas del Toro*	09.20 N – 82.15 W	11	11
Venezuela	Higuerote	10.32 N – 66.05 W	9	19
	Isla Tortuga	10.54 N – 65.12 W	10	
Guadeloupe	La Manche à Eau	16.16 N – 61.33 W	10	10
Brazil	Recife *	08.05 N – 34.53 W	1	9
	Ilha Itaparica	13.02 S – 38.47 W	8	
			Total:	98

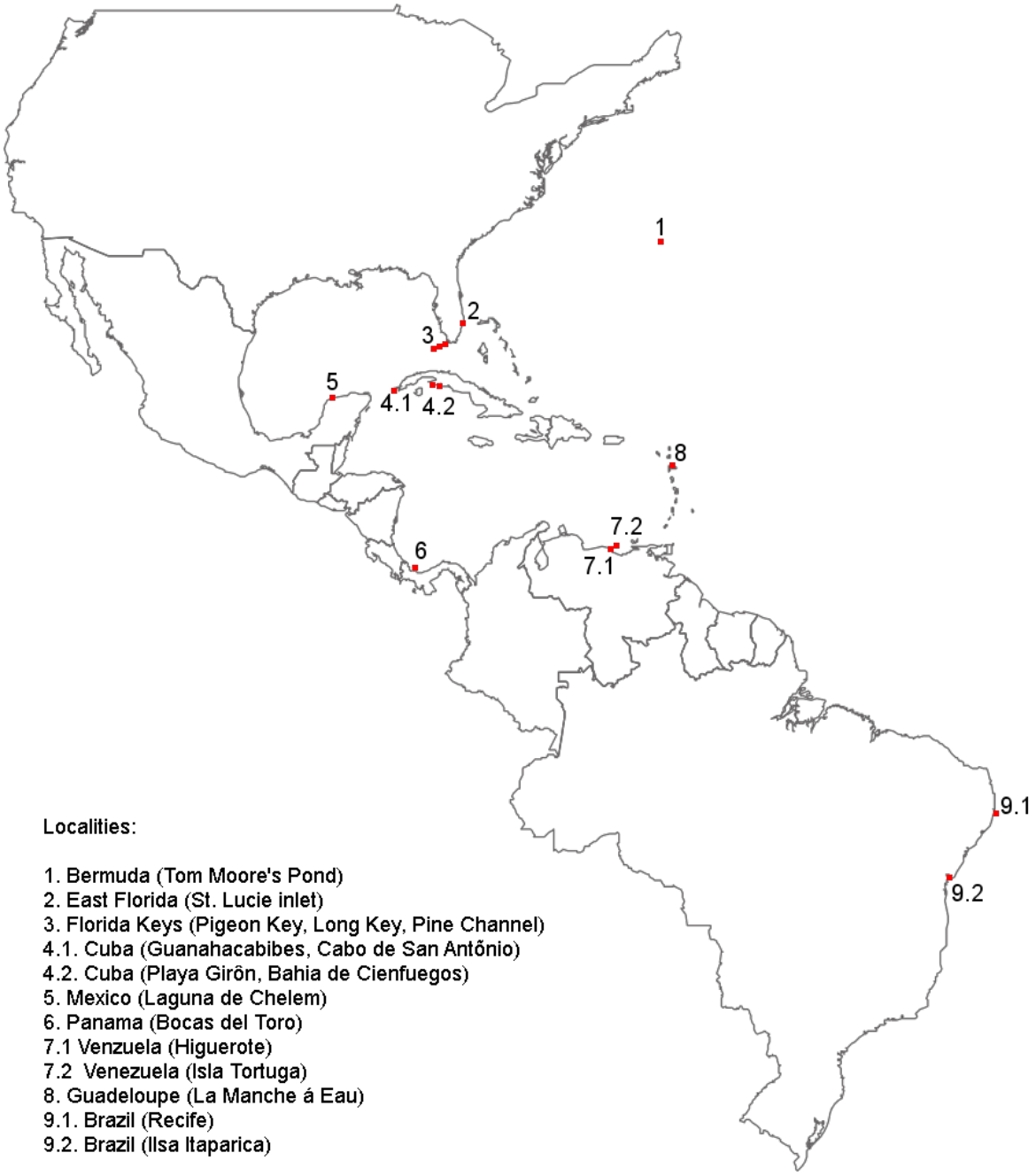

Figure 4: *Bulla occidentalis* sample distribution. Red dots indicate sampling stations.

3.2. DNA extraction, PCR and sequencing

Total genomic DNA was extracted using foot tissue, or in cases with very small specimens, shells were broken and whole specimens were used. Extractions were made using the Quiagen DNeasy Blood and Tissue Kit following the manufacturers protocol Purification of Total DNA from Animal Tissues (Spin-Column Protocol) (Qiagen, Valencia, CA, USA; 09/2001). Tissue was lysed overnight on a heated platform instead of the 1-3 hours as suggested by the protocol, and only steps 1-7 were

performed to produce 200 µL of total genomic DNA extract. The steps are as follows: 1 - 2) lysis of approximately 25 mg of tissue in 180 µL Qiagen ATL-buffer and 20 µL Qiagen proteinase-K, 3) 15 second vortexing and adding of 200 µL of each of Qiagen AL-buffer and 96% ethanol, 4) pipet mixture into a Qiagen Dneasy spin-column placed in a 2 mL collection tube and centrifuge at 8000 rpm for 1 minute, 5) discard flow-through and collection tube and place spin column in new collection tube before adding 500 µL Qiagen AW1-buffer and centrifuging for 1 minute at 8000 rpm, 6) discard flow-through and collection tube and place spin column in new collection tube before adding 500 µL Qiagen AW2-buffer and centrifuging for 3 minutes at 14000 rpm, 7) place spin-column in 1,5 mL microcentrifuge tube before pipetting 200 µL Qiagen AE-buffer, incubate the sample at room temperature for 1 min before centrifuging for 1 minute at 8000 rpm, 8) repeat step 7.

Approximately 700 bp COI DNA was amplified in 50 µL reactions containing 17,5 µL Sigma Water, 5 µL Qiagen 10X PCR Buffer, 5 µL 2 µM dNTPS's, 10 µL Qiagen Q-solution, 7 µL 25 mM $MgCl_2$, 2 µL 10 µM of each of the primers HCO2198 and LCO1490 (Folmer *et al.* 1994), 0,5 µL Qiagen Taq DNA Polymerase and 1 µL DNA-extract pr. sample. Sequences were amplified with an initial denaturation phase of 95°C for 3 minutes, followed by 40 cycles with a 45 second 94°C denaturation phase, a 45 second 45°C annealing phase and a 2 minute 72°C extension phase. The program was finalized with 10 minutes at 72°C. Some of the COI-PCRs were performed using the Qiagen HotStart$^+$ TAQ polymerase, for which the initial denaturation phase was prolonged from 3 to 5 minutes.

Approximately 500 bp of the mitochondrial 16S-rRNA gene was amplified using the same amounts of reagents as for COI, the only differences being the primers. The primers used for 16S PCRs were 16Sar-L and 16Sbr-H (Palumbi 2002). Qiagen HotStart$^+$ TAQ polymerase was used for all 16S-PCRs. Sequences were amplified with an initial denaturation phase of 95°C for 5 minutes, followed by 39 cycles with a 45 second 94°C denaturation phase, a 45 second 51,5°C annealing phase and a 2 minute 72°C extension phase. The program was finalized with 10 minutes at 72°C. See Table 3 for primer details.

Table 3: Primer information

Primer name	Primer sequence	Publication
LCO1490	5'-GGTCAACAAATCATAAAGATATTGG-3'	Folmer *et al.* 1994
HCO2198	5'-TAAACTTCAGGGTGACCAAAAAATCA-3'	Folmer *et al.* 1994
16Sar-L	5'-CGCCTGTTTATCAAAAACAT-3'	Palumbi 2002
16Sbr-H	5'-TGCACTAGACTCAAGTCTGGCC-3'	Palumbi 2002

Problematic DNA-extracts that did not yield satisfactory PCR products were diluted 50 times with Quiagen Buffer AE (1 µL DNA Extract, 49µL buffer). This diluted DNA-extract was amplified using the same amount of reagents as before. The original extracts for the samples that did not yield good PCR product after this treatment were concentrated using a vacuum-centrifuge until the total volume was reduced from around 200 µL to between 10 and 50 µL. 1 µL of this concentrate was then used for new PCRs reactions. As a last resort Quiagen REPLI-g (Qiagen, Valencia, CA, USA; 10/2006) was used to amplify total genomic DNA.

The quality of PCR products was assessed using gel electrophoresis imaging with a 1% agarose gel and 0,5 M TBE buffer solution. 1 µL of loading buffer was used with 4 µL PCR product. Gel-electrophoresis images and manual band-quantification was performed using the GeneTools package from Syngene (Synoptics Limited, Beacon House, Nuffield Road, Cambridge CB4 1TF, United Kingdom).

Sequences were purified in 40 µL reactions each containing 0,4 µL EXO1 (10 U/µL), 4,0 µL SAP (10 U/µL) and 3,6 µL Sigma Water in addition to 32 µL PCR product. This was run through the thermal cycler at 37°C for 30 minutes and 85°C for 15 minutes. Two different PCR-cycler machines were used for all amplification and purification of samples. These were an Eppendorf Mastercycler ProS and a Bio-Rad C1000 Thermal Cycler.

The majority of DNA sequencing was performed by Macrogen Inc. (908 World Meridian Venture Center, #60-24, Gasan-dong, Geumchun-gu, Seoul 153-781, Korea) with purified PCR products varying between 2 and 55 ng/L of DNA. All PCR products were sequenced in two directions using the same primers as used in the PCR reactions. Occasionally, the local sequencing-lab at the Institute for Molecular Biology, University of Bergen was used in cases where only few samples were available sequencing or to test the quality of the results. For these sequences the sequencing

reactions were prepared using a Big-Dye v3.1. The protocol included using 10 ng template DNA, 1 µL Big-Dye, 1 µL Sequencing buffer, 3,2 pmol Primer and water up to a total volume of 10 µL. The sequencing-reaction was run in a PCR-cycler with the following conditions: An initial step of 96º C for 5 min followed by 25 cycles of 96ºC for 10 sec, 50 º C for 5 sec and 60ºC for 4 min. 10 µL of water was added to the reactions before delivery to the sequencing facility.

3.3. DNA analyses

3.3.1. Assembly and alignment

Sequences were assembled from forward and reverse primers using Sequencher v4.10.1 (Gene Codes Corporation) and were aligned together with the sequences downloaded from GenBank (Appendix I) using ClustalX v2.0 (Larkin *et al.* 2007) before being manually inspected and adjusted in BioEdit v7.0.5.3 (Hall 1999). BioEdit v7.0.5.3 (Hall 1999) was used for trimming sequences prior to analysis.

3.3.2. Molecular clocks

The assumption that the COI and 16S mitochondrial genes evolved under a strict molecular clock was assessed using model parameters from two Bayesian tree searches, set up as in section 3.3.4., and inspected in Tracer v1.5 (Drummond and Rambaut 2007). The first run used the combined dataset with outgroup and a Yule prior for speciation, and the second run excluded the outgroup and used a Bayesian Skyline coalescent prior. The parameter ucld.stdev can be used to assess the behaviour of substitution rates in the dataset. If this value is zero there is no variation in rates among branches, but if this value becomes larger than 1, the standard deviation in branch rates is greater than mean rates, and rate heterogeneity can be expected. In addition, if the distribution of estimated substitution rates abbute against zero there is no among-branch rate heterogeneity. This also applies to the coefficient of variation-parameter (Drummond *et al.* 2007).

3.3.3. Population genetics

In all analyses falling under the population genetics heading the sequence Cuba074 was excluded due to one nucleotide ambiguity (IUPAC ambiguity code R). When describing population genetics

analyses the term population will be used to describe all sequences falling into one sampling country (Table 2), meaning that specimens from for instance Venezuela will fall into one Venezuelan population even though there are two sampling stations in this country.

Standard genetic diversity-calculations were performed in Arlequin v3.5.1.2 (Excoffier and Lischer 2010). The statistics include number of haplotypes (Nh), haplotype diversity (h), number of polymorphic sites (Np), nucleotide diversity (π_n) and mean number of pairwise differences between sequences (k) in each of the populations. This was done for each of the individual genes and for the combined dataset. This software was also used for calculating pairwise population F_{ST} and population Φ_{ST} values to assess the degree of subdivision within the TWA. Pairwise F_{ST} values represent comparisons between pairs of populations and provide information on the degree of differentiation between populations. Significance tests are performed with 5000 permutations under the null hypothesis that there are no differences between populations. The obtained p-value is the proportion of permutations that provide an F_{ST}-value that is larger than the observed value (Excoffier and Lischer 2010). Φ_{ST} is a fixation index measured through Analysis of Molecular Variance (AMOVA) and this was used to assess hierarchical population structure by computing the degree of explained variability within and between groups of populations based on a priori assumptions of groups. These analyses were set up to: 1) test the hypothesis of one panmictic TWA-population 2) test the hypothesis of four connectivity regions corresponding to: Eastern Caribbean, Western Caribbean, the Bahamas-region and the coastlines influenced by the Colombia-Panama gyre (Cowen *et al.* 2006). The significance of the test was assessed by performing 20000 permutations of the underlying data and recomputing statistics to create a null distribution. The assumption of normal distribution and equality of variance in the populations is not necessary in AMOVA as implemented in Arlequin v3.5.1.2 because of null-distributions from permutations (Excoffier and Lischer 2010).

Haplotype networks for COI and 16S were created using TCS v1.21 (Posada and Crandall 2000) with default settings and treating insertions and deletions as a fifth state. We also tested for neutrality using standard tests, Tajima's D and Fu's Fs in Arlequin v3.5.1.2 (Excoffier and Lischer 2010). p-values for Tajima's D and Fu's Fs were calculated with 10000 permutations to asses statistical significance. This process generates random samples under the hypothesis of neutrality and a population in equilibrium with the use of a coalescent simulation algorithm (Excoffier and Lischer 2010). Both Tajima's test and Fu's Fs are based on an infinite-site model without

recombination, and significance is tested by generating random samples (permutations) of the samples under the hypothesis of selective neutrality and a population in equilibrium, with the use of a coalescent simulation algorithm.

3.3.4. Phylogenetic analysis and estimating divergence times

Appropriate nucleotide substitution models were selected with the software MEGA 5.0 (Tamura *et al.* 2011) according to the Akaike Information Criterion. The selected model for COI was the HKY+G+I and for 16S the GTR+G model was selected (see Appendix II for details). Using the same software, the substitution saturation of first second and third codon positions in the COI gene was visually inspected both including and excluding an outgroup in the dataset. This was done by plotting total number of sequence differences (transitions + transversions) against pairwise *p*-uncorrected distances for each of the codon positions. The intraspecfic phylogeny of *B. occidentalis* was inferred using a Bayesian Markov-Chain Monte Carlo (MCMC) analysis in Beast v1.6.1 (Drummond and Rambaut 2007). This was done separately for each gene to assess the congruence of gene tree topologies. Searches ran for ten million generations with sampling every 1000 generations. The first 100 trees in each run were discarded as burn-in after visual inspection of convergence in Tracer v1.5 (Drummond and Rambaut 2007). The tree searches were set up in Beauti v1.6.1 (Drummond and Rambaut 2007) using the same settings as for the combined dataset, which will be described next.

Based on the combined dataset the genealogy and divergence times were estimated in Beast v1.6.1 (Drummond and Rambaut 2007) using two *B. striata* sequences as an outgroup (16S: DQ986625, DQ986631, COI: DQ986564, DQ986566). The run was set up in Beauti v1.6.1 (Drummond and Rambaut 2007) with data partitioned into two genes with the nucleotide substitution-models as found in MEGA 5.0 (HKY+I+G for COI, GTR+G for 16S), but the tree priors were linked to reflect the fact that the non-recombining mitochondrial genome in reality is one locus and therefore the genes are expected not to have significantly different genealogies. Substitution models and clock rates were unlinked, and a Yule-prior for speciation was used because we included an outgroup from another species. The tree root height prior was set up with a lognormal distribution. The lognormal distribution is considered to be appropriate for fossil calibrated phylogenies because it incorporate the uncertainty related to fossil age estimates and the fact that fossils can only provide minimum age estimates (Forest 2009). The lognormal distribution was set up with a mean of 18.2

Mya, a ln standard deviation of 0.066 and an offset of 0, yielding a 2.5% quantile of 15.96 Mya and a 97.5% quantile 20.67 Mya. These priors were based on fossils of *B. chipolana* which is to our best knowledge the earliest fossil sharing synapomorphic traits with *B. occidentalis.* These fossils are known from the Chipola formation in Florida, USA, and date to the Burdigalian in the Early Miocene (20.43 – 15.97 Ma) (Huddlestun 1984; Weisbord 1971). We let the two genes evolve under the assumption of a strict molecular clock as suggested by test parameters from Beast under different models (see Results). The substitution rate was allowed to be estimated for both genes with uniform priors in the range 0-10 for both with a 0.1 initial value for COI and a 0.01 initial value for 16S. This was based on prior knowledge about substitution rates in *Bulla spp*. (COI: 0.5% My^{-1} and 16S: 0.05% My^{-1}) (Malaquias and Reid 2009). The Bayesian MCMC analysis was run for twenty million generations with sampling every thousand generations. The computations were performed in Beast v1.6.1 (Drummond and Rambaut 2007). The parameter log file was visually inspected in Tracer v1.5 (Drummond and Rambaut 2007). TreeAnnotator v1.6.1 (Drummond and Rambaut 2007) was used to produce a consensus maximum clade credibility tree with mean node heights from the stored trees from the MCMC run with a 10% burn-in fraction.

3.3.5. Demographic history of B. occidentalis

The demographic history of *B. occidentalis* in the period after the three main lineages split at 11,06 – 6,11 Mya as inferred from the species genealogy (see Results) was estimated using Beast v1.6.1 (Drummond and Rambaut 2007). The reconstruction of demographic history based on a genealogy is subjected to a large degree of uncertainty (Ho and Shapiro 2011), and this problem is adressed in the Bayesian Skyline method where the genealogy, the demographic history and parameters in the substitution models are co-estimated in one single analysis together with credibility intervals that represent phylogenetic and coalescent uncertainty. This should therefore minimize the errors as far as possible (Ho and Shapiro 2011).

The run was set up in Beauti v1.6.1 (Drummond and Rambaut 2007) with data partitioned into two genes with the nucleotide substitution-models as found in MEGA 5.0 (HKY+I+G for COI, GTR+G for 16S), but the tree priors were linked. As tree prior, we used the Coalescent Bayesian Skyline, and default priors were used for the rest of the parameters except for the tree root height, molecular clocks and skyline population size. The coalescent framework implies assumptions about the dataset: ideally the sequences should be gathered randomly from a panmictic population, the

markers should be orthologous, non-recombining and should evolve neutrally (Drummond *et al.* 2005). The piecewise-constant model embedded in the analysis assumes that population size is constant in any one time interval and changes instantaneously at the transition between two intervals (Ho and Shapiro 2011). Selecting the correct number of groups (i.e. intervals) is at this point not a simple task because of the lack of thorough guidelines (Ho and Shapiro 2011). The default number of ten groups was selected based on what is used in a similar study with a dataset of comparable size (Cunha *et al.* 2011) and based on advice from the developers of the methodology (Simon Ho, personal communication).

The tree root height prior was set up based on the divergence times estimated from the analysis in section 3.3.4. The lognormal distribution was set up with a mean of 8,5 Mya, a ln standard deviation of 0,155 and an offset of 0,5, yielding a 2.5% quantile of 6,197 Mya and a 97.5% quantile 11,38 Mya. We let the two genes evolve under the assumption of a strict molecular clock as suggested by test parameters from Beast under different models (see Results) and because we are dealing with an intra-specific genealogy, it is unlikely that there is considerable variation between lineages. The substitution rate was allowed to be estimated with uniform priors in the range 0-10 for both with a 0.1 initial value for COI and a 0.01 initial value for 16S. The population size prior was set to a uniform distribution with a lower bound of 1 and an upper bound of 10^9 and a starting value of 1. Little is known about the size of the *B. occidentalis* population in the TWA, and we therefore chose to use a generous upper bound to avoid restriction of the effective population size estimate. The Bayesian MCMC analysis was run for 10 million generations with sampling every thousand generations. The computations were performed in Beast v1.6.1 (Drummond and Rambaut 2007). The demographic history was inferred from a Bayesian Skyline Plot (BSP) produced using Tracer v1.5 (Drummond and Rambaut 2007) with a 10% burn-in fraction.

3.3.6. Isolation-by-distance

Correlation between genetic differentiation and geographic distance was assessed using the Isolation-by-distance web-service (Jensen *et al.* 2005). All distinct sample localities were treated as populations, so that for instance Cuba had two populations (Cabo de San Antonio and Playa Giron). All sample sites with only one individual were excluded from the analysis because limitations in the software allow only one such population. This included Bahia de Cienfuegos, Recife, Guanahacabibes and Pigeon Key. The Isolation by Distance-analysis was set up with the following

settings: 10000 randomizations for testing statistical significance, genetic distances measured as F_{ST} and gaps ignored. Statistical significance was tested by a Mantel test, to assess if the pairwise genetic distance-matrix was correlated with the pairwise geographical distance-matrix, as well as linear regression (Bohonak 2002). All distances were measured using Google Earth (http://www.google.com/earth/index.html).

Two different analyses were performed; one with straight-line distances between sites and one with approximate distances along the trajectories of ocean surface currents connecting the sites. Measuring distances in straight lines between sites is, of course, unrealistic as the effective distance between two localities in the ocean cannot be measured across land, but this method was chosen because it does not require subjective opinions about travel routes.

Some assumptions were made for the analysis using distances along hypothetical dispersal routes. Based on general current patters (Figure 1) it was assumed that Brazil, East Florida, Guadeloupe and Bermuda were most plausibly connected without implying dispersal through the entire Caribbean Sea and instead measure distance on the outside of the Antilles Arc. The extremely large distances resulting from Carribbean Sea dispersal-routes and the possibility of the Antilles current acting as a connective force suggests that this is a plausible connective pattern. As the approximated oceanographic distances are approximations and may be unrealistic, this test was performed to investigate whether correlation is improved by scaling geographic distances. See Appendix II for distance matrices.

4. RESULTS

4.1. Sequence analysis

Including the sequences from GenBank, our dataset numbered a total of 98 sequences with 571 bp for COI and 98 sequences with 387 bp for 16S. Both COI and 16S were successfully sequenced for all samples, yielding a 958 basepair long concatenated alignment of 98 sequences. One of the sequences (Cuba074) had one ambiguous position (IUPAC ambiguity code R) and was included in the phylogenetic analysis and the reconstruction of demographic history, but excluded from all population genetic analyses. See Table 2 for overview of sampling localities and Appendix I for full specimen list.

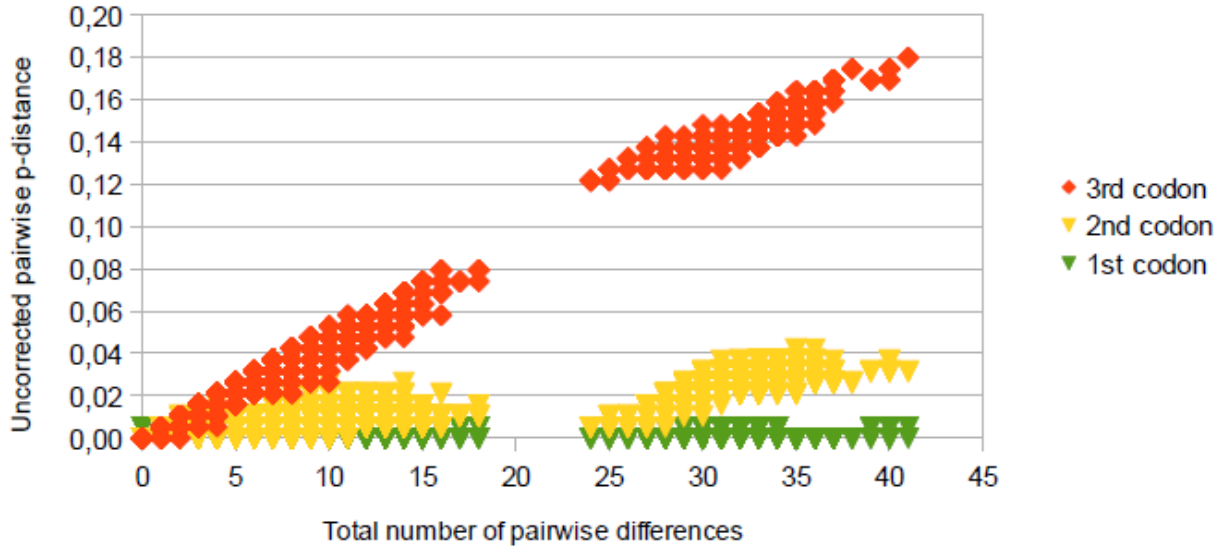

Figure 5: Substitution saturation plot

Saturation in the third codon position for COI was assessed by plotting total number of pairwise differences (transitions and transversions) against uncorrected *p*-distances for each of the codon positions. No evidence for saturation was was found both when including and excluding the outgroup in the analysis. Figure 5 shows the saturation-plot for the dataset excluding outgroup. The plot shows that the third codon position *p*-distances do not flatten out with increasing total distance, as would be expected in cases where saturation is taking place.

A plot of pairwise uncorrected *p*-distances for COI shows a bimodal distribution (Figure 6) with most distances falling into the intervals 0,0% – 2,5% and 4,5% – 6,5%. This could indicate that

there are at least two differentiated sets of sequences for which within-set distances are greater than between-set distances.

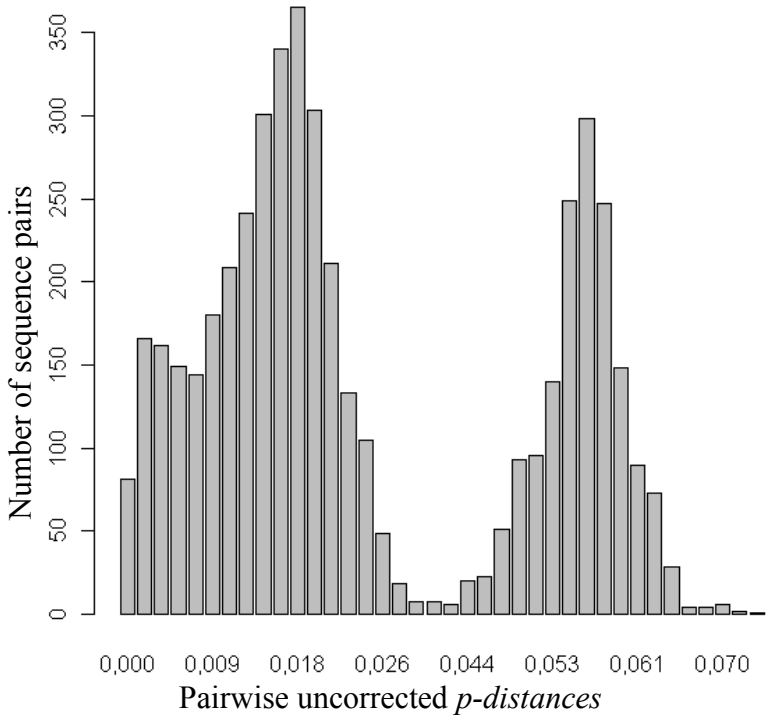

Figure 6: Histogram of pairwise uncorrected p-distances

4.2. Molecular clocks

Inspection of test parameters in Tracer v1.5 (Drummond and Rambaut 2007) suggested that the dataset evolved under a strict molecular clock (Table 4). 16S lies consistently below 0,5 for both parameters for both genes in the two different models. COI, on the other hand, shows high values under the model using a Yule speciation prior, but small values under the Bayesian Skyline Coalescent Model. Because only one of the parameters is slightly above one, the strict clock model will be used as it is likely that substitution rates will be similar between intra-specific lineages.

Table 4: Molecular clock parameters

		COI	16S
Outgroup / Yule prior	ucld.stdev	0,9820	0,308
	coefficient of variation	1,142	0,3135
No outgroup / Bayesian Skyline Model Prior	ucld.stdev	0,2116	0,4070
	coefficient of variation	0,2094	0,4251

4.3. Population genetic structure

For all population genetics-related analyses the sequence Cuba074 was left out because of an ambiguous position and the fact that ambiguities are not supported for some software packages. This left us with a dataset of 97 sequences of 958 bps for population genetic analyses. When discussing population genetic analyses, the term population will be used for describing all sampling localities from one country as evident from Table 2.

Table 5 sums up standard diversity indices for the two genes and combined dataset for each of the populations. COI is generally more variable than 16S, with a higher haplotype-diversity for all populations, often several times higher. COI has a haplotype-diversity that varies from 0,6667 – 1,0 within populations while 16S haplotype-diversity varies between 0,0 – 0,7912. A haplotype-diversity of 1,0 essentially means that all specimens from that locality are different while a haplotype diversity of 0,0 means that all sequences from a single locality share the same haplotype. The COI nucleotide-diversity varies between 0,002484 to 0,010819 while it varies between 0,0 and 0,006719 for 16S. This means that most of the variety in this dataset comes from COI. This is also evident from the fact that the COI gene has 60 and 16S only has 22 unique haplotypes out of a total of 97 sequences.

Table 5: Standard diversity indices
n = number of sampled individuals, Nh = number of haplotypes, h = haplotypic diversity, Np = number of polymorphic sites, π_n = nucleotide diversity, k = mean number of pairwise difference

Gene	Site	n	Nh	*h*	Np	π_n	k
COI	Bermuda	8	4	0.7857 ± 0.1127	11	0.009882 ± 0.006040	5.642857 ± 3.027684
	East Florida	14	9	0.9341 ± 0.0448	43	0.024480 ± 0.013128	13.978022 ± 6.677808
	Florida Keys	6	5	0.9333 ± 0.1217	7	0.004086 ± 0.002984	2.333333 ± 1.475730
	Cuba	12	5	0.6667 ± 0.1409	32	0.009579 ± 0.005583	5.469697 ± 2.831432
	Mexico	8	4	0.7500 ± 0.1391	6	0.003878 ± 0.002718	2.214286 ± 1.362307
	Panama	11	6	0.7273 ± 0.1444	7	0.002484 ± 0.001850	1.418182 ± 0.936320
	Venezuela	20	14	0.9474 ± 0.0344	35	0.009264 ± 0.005216	5.289474 ± 2.666604
	Guadeloupe	10	10	1.0000 ± 0.0447	26	0.010819 ± 0.006354	6.177778 ± 3.208330
	Brazil	9	6	0.8333 ± 0.1265	8	0.003113 ± 0.002248	1.777778 ± 1.131547
16S	Bermuda	8	3	0.6786 ± 0.1220	4	0.005089 ± 0.003655	1.964286 ± 1.238432
	East Florida	14	6	0.7912 ± 0.0894	10	0.006719 ± 0.004294	2.593407 ± 1.476400
	Florida Keys	6	2	0.3333 ± 0.2152	1	0.000864 ± 0.001137	0.333333 ± 0.380058
	Cuba	12	2	0.1667 ± 0.1343	6	0.002584 ± 0.002102	1.000000 ± 0.722435
	Mexico	8	1	0.0000 ± 0.0000	0	0.0000 ± 0.0000	0.0000 ± 0.0000
	Panama	11	4	0.4909 ± 0.1754	4	0.002261 ± 0.001933	0.872727 ± 0.661436
	Venezuela	20	6	0.4474 ± 0.1367	7	0.002277 ± 0.001859	0.878947± 0.642503
	Guadeloupe	10	3	0.3778 ± 0.1813	3	0.001554 ± 0.001521	0.600000 ± 0.519281
	Brazil	9	3	0.5556 ± 0.1653	3	0.002447 ± 0.002088	0.944444 ± 0.710412
Combined	Bermuda	8	4	0.7857 ± 0.1127	15	0.007949 ± 0.004729	7.607143 ± 3.973043
	East Florida	14	10	0.9451 ± 0.0451	53	0.017316 ± 0.009216	16.571429 ± 7.857279
	Florida Keys	6	6	1.0000 ± 0.0962	8	0.002786 ± 0.001987	2.666667 ± 1.646545
	Cuba	12	5	0.6667 ± 0.1409	38	0.007133 ± 0.004068	6.833333 ± 3.461689
	Mexico	8	4	0.7500 ± 0.1391	6	0.002314 ± 0.001622	2.214286 ± 1.362307
	Panama	11	6	0.7273 ± 0.1444	11	0.002394 ± 0.001601	2.290909 ± 1.358171
	Venezuela	20	15	0.9579 ± 0.0328	37	0.006446 ± 0.003572	6.168421 ± 3.060647
	Guadeloupe	10	10	1.0000 ± 0.0447	29	0.007082 ± 0.004124	6.777778 ± 3.490018
	Brazil	9	7	0.9444 ± 0.0702	11	0.9444 ± 0.0702	2.722222 ± 1.591853

Tajima's D was negative for both genes meaning there is an excess of low frequency polymorphisms, which can indicate that both genes are under purifying selection (Haubold and Wiehe 2006) (Table 6). However the *p*-values are high showing no statistical significance of the result. Fu's Fs is negative for both genes, with a larger negative value for COI. Negative Fs-values are considered to be evidence for excess alleles and therefore recent population expansions (Excoffier and Lischer 2010; Fu 1997). P-values for Fu's Fs are significant on a 0,05 significance level. This means that our sequences cannot be viewed as behaving neutrally, but rather as evidence

of a recent population expansion.

Table 6: Neutrality tests

COI			
Tajima's D	P-value	Fu's Fs	P-value
-0.42107	0.38930	-22.09795	0.00080
16S			
Tajima's D	P-value	Fu's Fs	P-value
-1.02694	0.15200	-7.61527	0.00930

Pairwise F_{ST} values are summarized in Table 7. This shows the size of the interpopulation genetic variation for population pairs compared to the intrapopulation variation. The values range from 0,10007 – 0.94130 with some localities scoring constantly high values while others are more varied. Cuba and Florida Keys stand out with consistently high values while the other groups vary throughout. This implies that these populations are the most differentiated from the rest and is in line with the groupings retrieved from phylogenetic analyses. One non-significant *p*-value is marked in bold.

Table 7: Mean pairwise F_{ST}'s (below diagonal) and *p*-values (above diagonal)

	Bermuda	**Brazil**	**Cuba**	**East Florida**	**Florida Keys**	**Guadeloupe**	**Mexico**	**Panama**	**Venezuela**
Bermuda		0.0±0.0	0.0±0.0	0.01032 ± 0.0013	0.0±0.0	0.0±0.0	0.0±0.0	0.0±0.0	0.0±0.0
Brazil	0.36583		0.0±0.0	0.0±0.0	0.00040 ± 0.0003	0.00040 ± 0.0003	0.0±0.0	0.0+-0.0	0.0±0.0
Cuba	0.79000	0.83923		0.0±0.0	0.00060 ± 0.0003	**0.08788 ± 0.0044**	0.0±0.0	0.00020 ± 0.0002	0.0±0.0
East Florida	0.12338	0.31359	0.62758		0.00040 ± 0.0003	0.00040 ± 0.0003	0.0±0.0	0.0±0.0	0.00020 ± 0.0002
Florida Keys	0.85497	0.92264	0.82571	0.69436		0.0±0.0	0.0±0.0	0.0±0.0	0.00020 ± 0.0002
Guadeloupe	0.44471	0.61031	0.80787	0.19388	0.86458		0.0±0.0	0.0±0.0	0.03848 ± 0.0027
Mexico	0.48980	0.71819	0.85742	0.10689	0.93821	0.41151		0.0±0.0	0.0±0.0
Panama	0.44014	0.82753	0.87005	0.30467	0.94130	0.70167	0.81427		0.0±0.0
Venezuela	0.42988	0.58051	0.81763	0.20589	0.86335	0.10007	0.35259	0.65074	

The AMOVA testing the hypothesis of one panmictic TWA-population was designed with all sampling populations in one group, and test parameters and results can be found in Table 8. It is evident from this that the largest variance component is explained among populations (68%), meaning that within-population variation is generally less than between populations. This could be

an indication of geographical structure in the TWA-population rather than panmixia.

Table 8: AMOVA results for hypothesis of panmictic population

Source of variation	Degrees of freedom	Sum of squares	Variance components	Percentage of variation
Among populations	8	532.627	5.95687	68.26
Within populations	89	246.526	2.76995	31.74
Total	97	779.153	8.72683	
Fixation index (Φ_{ST})	0.68259	p < 0,05		

An AMOVA-analysis was set up to test the "connectivity-hypothesis" suggested by Cowen *et al.* (2006). In this analysis five groups represented the four connectivity regions (Eastern Caribbean, Western Caribbean, the Bahamas-region and the coastlines influenced by the Colombia-Panama gyre) and Brazil in a group of its own since it did not fall into any of the four connectivity regions. The largest variance component is explained by variation among populations within groups, and if the connectivity-regions were to apply to *B. occidentalis* we would expect the most explained variance among groups (Table 9). 64.92 % of the variation is explained at the among-population level with a $p < 0.05$, while 32% is explained within populations within groups with a $p < 0.05$. The subdivision of the population into groups does not markedly change the results from the AMOVA, and the inter- and intra-population variance components are similar in magnitude.

Table 9: AMOVA results for hypotheses from Cowen *et al.* (2006) Groups: 1: Bermuda and East Florida. 2: Cuba, Florida Keys, Mexico. 3: Venezuela, Guadeloupe. 4: Brazil. 5: Panama

Source of variation	Degrees of freedom	Sum of squares	Variance components	Percentage of variation	Φ_{ST}	P
Among groups	4	335.450	0.25061	2.44	0.02444	P = 0,42
Among populations within groups	4	280.512	6.65648	64.92	0.67367	P < 0.05
Within populations	89	297.783	3.34587	32.63	0.66549	P < 0.05
Total	97	913.745	10.25297			

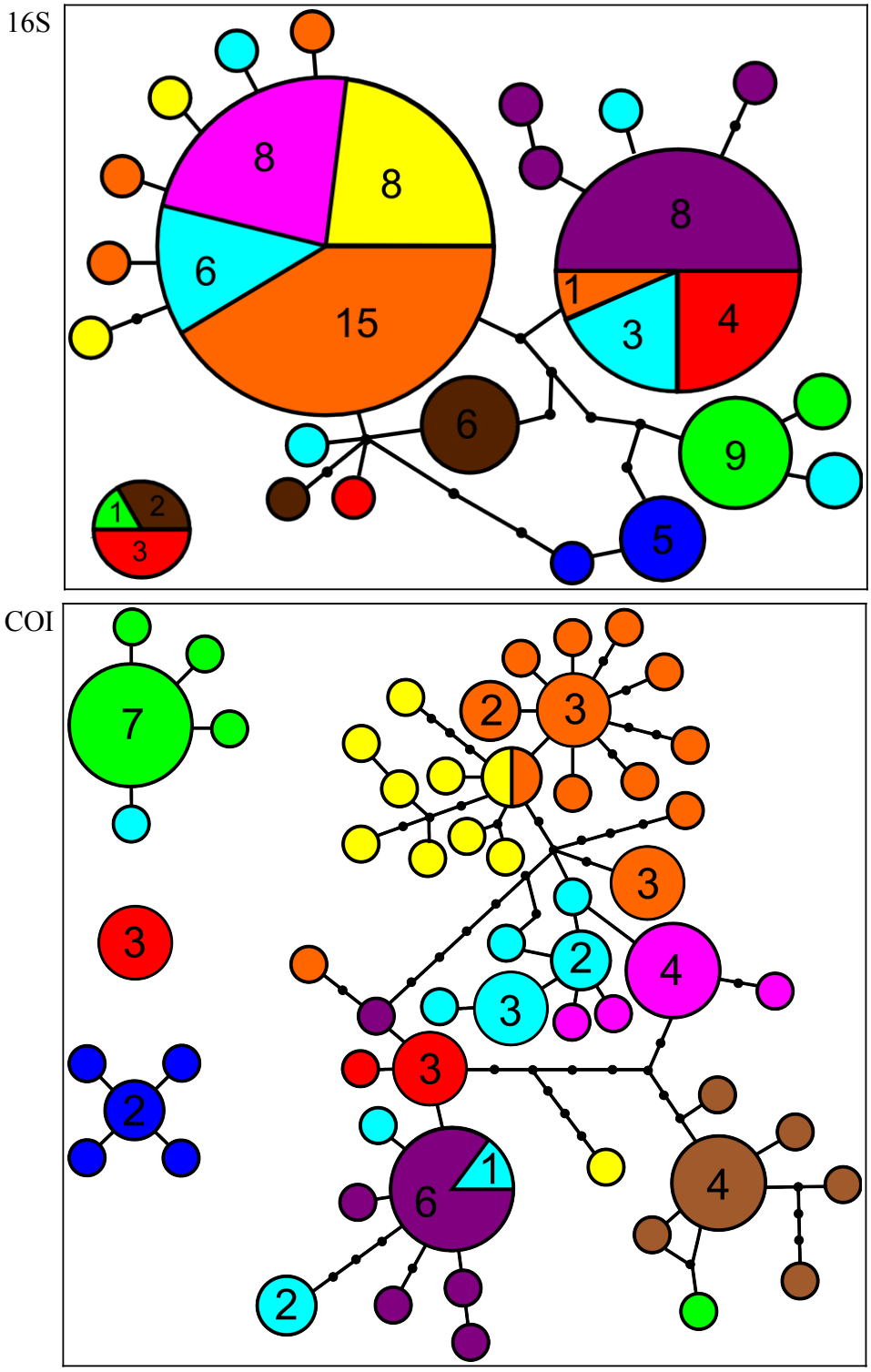

Figure 7: Haplotype-network. Top box: 16S, bottom box: COI. Size of circles correspond to number of sequences sharing that haplotype, also indicated by numbers. Lines connecting black dots represent mutational steps between haplotypes, while black dots represent theoretical intermediate haplotypes. Colour key; blue: Florida Keys, red: Bermuda, green: Cuba, cyan: East Florida, orange: Venezuela, yellow: Guadeloupe, purple: Panama, pink: Mexico, brown: Brazil.

4.4. Haplotype networks

The COI and 16S statistical parsimony haplotype networks created in TCS v1.21 (Clement *et al.* 2000) with a 95% connection limit are shown in Figure 7. The 95% connection limit equals 10 mutational steps, and is a cut-off value for the probability of parsimony. This means that connections in the network causing the probability of the total network to fall below a set threshold (95%) will cause these haplotypes to be represented in a separate network. The COI network consists of four distinct networks that are separated by the 95% connection limits. As can be seen from Figure 7, there are only very few shared haplotypes between populations. The 16S statistical parsimony network yielded two poorly structured networks, one encompassing most sequences, the other including Bermudan, Cuban and Brazilian sequences. The groups from the COI and 16S network do not correspond. Table 10 sums up uncorrected *p*-distances between the separate COI networks (A: the big network, B: the Florida Keys network (blue), C: the Cuban and East Floridian network (green and cyan), D: the Bermudan network (red)).

Table 10: Mean COI uncorrected *p*-distances for groups emergent from COI haplotype network. A: the big network, B: the Florida Keys network (blue), C: the Cuban and East Floridian network (green and cyan), D: the Bermudan network (red).

Groups	**Mean uncorrected *p*-distance**	Groups	**Mean uncorrected *p*-distance**
D / A	0,015	D / B	0,055
D / C	0,050	A / B	0,060
A / C	0,055	C / B	0,046

4.5. Phylogenetic analysis and estimating divergence times

COI, 16S and combined dataset phylogenetic trees all show the same three main lineages. These groups are: A) All sequences except those from Florida Keys, most from Cuba and two from East Florida, B) All Florda Keys sequences and C) All Cuban sequences except for two, and two East Floridian sequences. COI and 16S gene trees are presented in Appendix IV. The combined tree shows increased branch support values for the main groups, but, with an unsupported branching event separating lineage A from B and C. Mean COI uncorrected *p*-distances for the three groups are: AB: 0,059 ± 0,009, AC: 0,055 ± 0,008 and BC: 0,046 ± 0,008. In addition to large uncorrected *p*-distances between groups, these distances are large within groups. For instance group B has a range of uncorrected *p*-distances from 0,000 to 0,108 with a mean distance of 0,045.

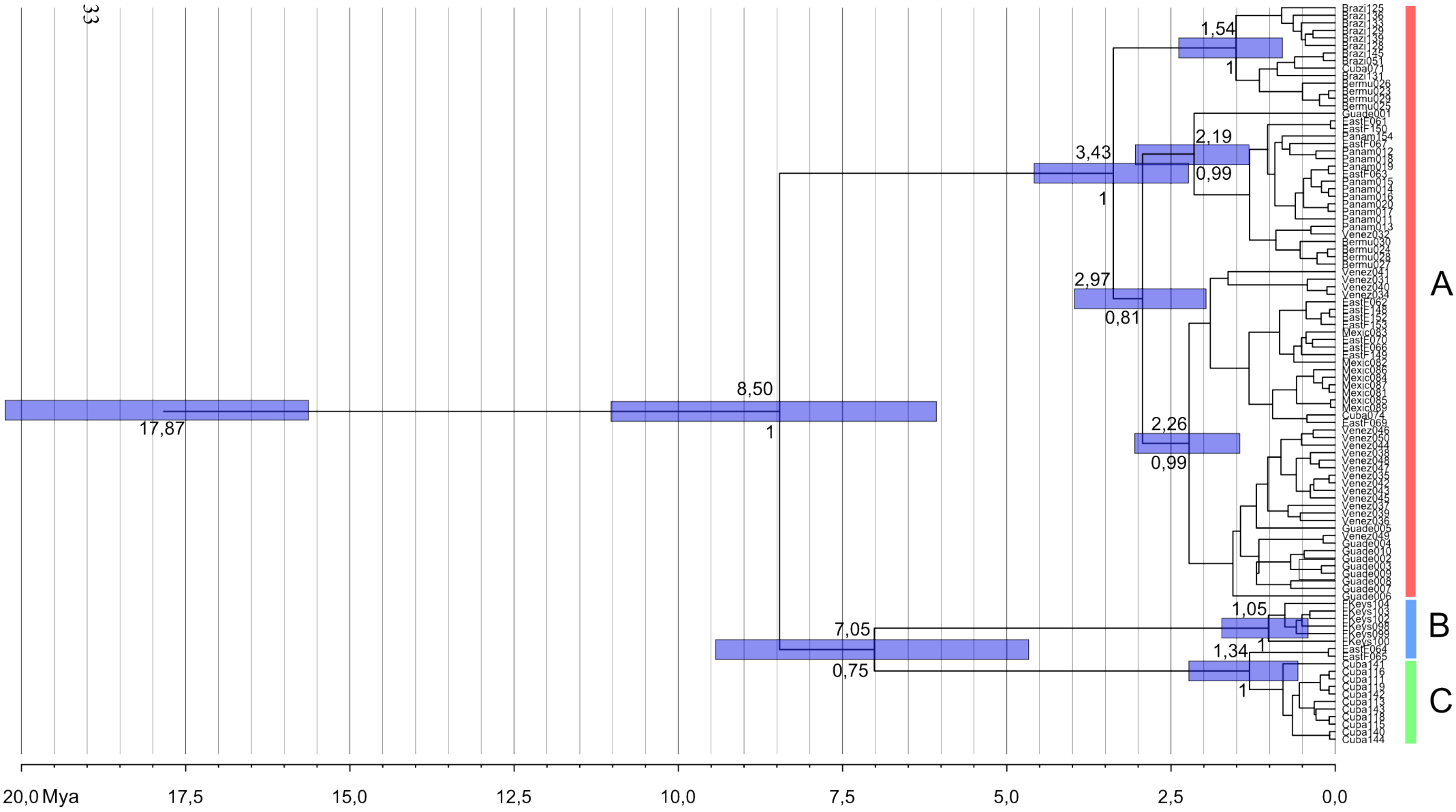

Figure 8: Chronogram showing divergence dates between *Bulla occidentalis* mitochondrial lineages based on COI and 16S genes. Node-ages are reported in million years before present, and blue bars are highest posterior density (HPD) intervals. The main groups (A, B and C) are indicated in the figure. Node ages are reported above and posterior probabilities below branches. Outgroup excluded from figure.

Table 11: Node ages in the *B. occidentalis* genealogy. See Figure 8 and text for clade definitions

Split	Age (Ma)
A / B / C	8,4952 (95% interval: 6,1077 / 11,0612)
B / A	7,0537 (unsupported)
Within A	3,4155 (95% interval: 2,2709 / 4,6219)
Within B	1,0454 (95% interval: 0,4506 / 1,7665)
Within C	1,3855 (95% interval: 0,6049 / 2,2661)

4.6. Demographic history

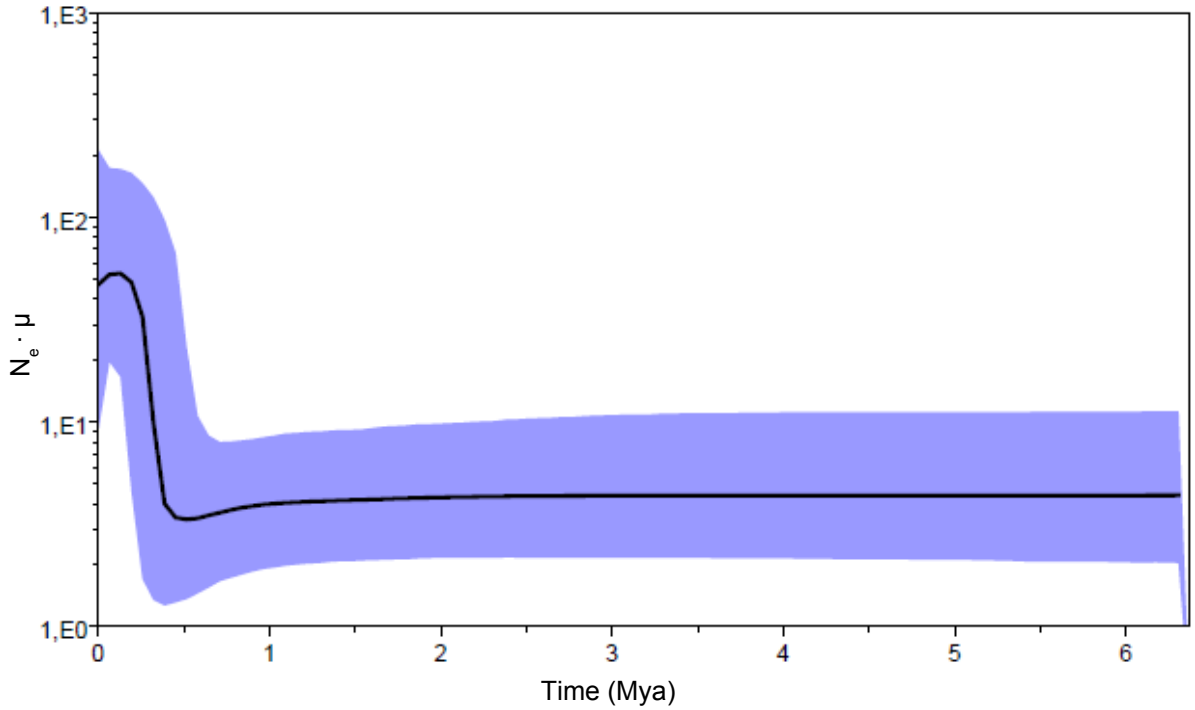

Figure 9: Bayesian skyline plot showing demographic history in the period after lineages split at 8.5 Mya in the *Bulla occidentalis* population. Black line indicates effective population size and blue fields indicate error margins. N_e = effective population size, μ = subtitution rate.

The Bayesian Skyline-Analysis showed that the population had a constant effective population size since the Late Miocene lineage division with a small bottleneck in the Lower Pleistocene followed by a marked population size expansion in the Middle and Upper Pleistocene (Figure 9).

4.7. Isolation by distance

Testing for isolation by distance showed no indications of a positive correlation between increasing

genetic distance with increased geographical distance. The two analyses yielded similar results, and both showed a slight negative relationship between geographic and genetic distances with small R^2-values indicating a weak relationship. The Mantel test showed that the null hypothesis of no correlation between geographic and genetic distance can not be rejected at the 0,05 significance level ($p_{straight}$ = 0,84, $p_{corrected}$ = 0,81). Test statistics are summarized in Table 12, and scatterplots of geographic against genetic distance are found in Figures 10 and 11.

Table 12: Isolation-by-Distance analyses: statistical results

Straight distances				
Mantel test	Z = 21.5253	r = -0.1878	p = 0.8441	
Linear regression	Intercept = 0.4049 ± 0.0368	Slope = -0.08276 ± 0.01019	R^2 = 0.0301	n = 66
Corrected distances				
Mantel test	Z = 27.1575	r = -0.1734	p = 0.8162	
Linear regression	Intercept = 0.4127 ± 0.0375	Slope = -0.1069 ± 0.0131	R^2 = 0.0353	n = 66

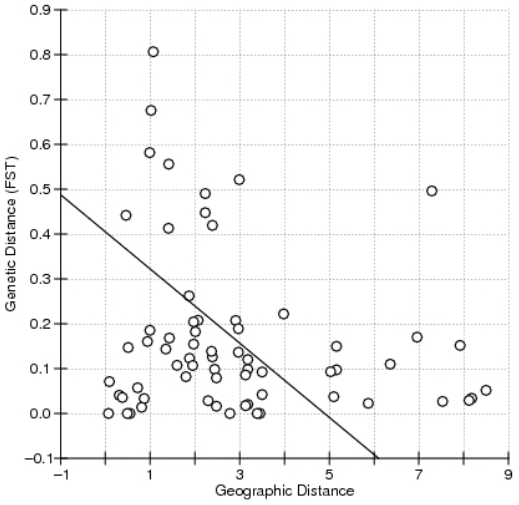

Figure 10: Isolation-by-distance plot with corrected oceanographic distances. X-axis scale: 1000 km.

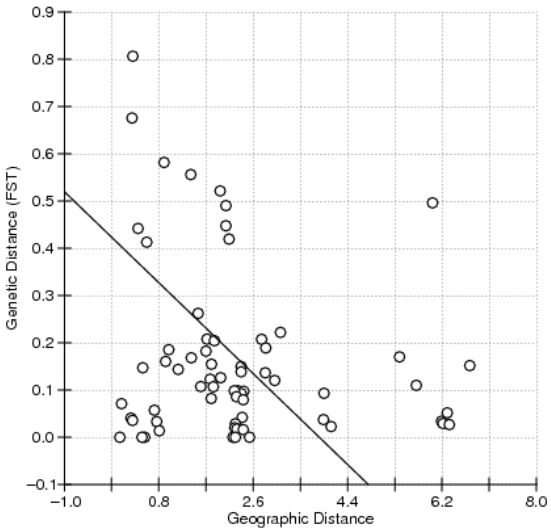

Figure 11: Isolation-by-distance plot with straight distances. X-axis scale: 1000 km.

5. DISCUSSION

5.1. Species genealogy and genetic diversity

The high genetic variability in *Bulla occidentalis* detected by Malaquias and Reid (2009) has to a large extent been confirmed by the presented results. This is evident both in the two gene trees (Appendix IV) as well as from the standard molecular diversity indices and the COI haplotype-network (Figure 7). The intra-specific phylogeny (Figure 8) retrieves three lineages (A, B and C), but only one of these is "geographically monophyletic" in the sense that it only includes sequences from one sampling population. This is the Florida Keys group (B), while the Cuban group (C) includes nearly all Cuban samples plus two sequences from East Florida. Despite being geographically proximate, they are genetically divergent and samples from these two clades have an average genetic distance of 4.6% (measured as average uncorrected *p*-distance for COI). The largest group (A) contains all other sequences including the two from Cuba that do not fall into clade C. Clade A has between 5–6% average genetic distance to clades B and C (measured as uncorrected *p*-distance for COI). These deep lineage splits within *B. occidentalis* support the hypothesis raised by Malaquias and Reid (2009) recognising three well-defined evolutionary significant units (ESUs) in the TWA.

The statistical parsimony haplotype networks (Figure 7) rendered four unconnected networks for the COI gene and two for 16S. Unconnected networks at the 95% connection limit have been taken as indications for the presence of cryptic species (Hart *et al.* 2006) which, based on the *B. occidentalis* haplotype networks could potentially suggest the presence of cryptic species in our dataset. Hebert *et al.* (2003) suggested that mean COI distance between sister species in molluscs to be 11,1 ± 5,1% (mean uncorrected *p*-distance), and that this could be used in DNA barcoding efforts. This percentage value was later considered to likely be inflated (Hart *et al.* 2006). The definition of this kind of threshold is ambiguous because different groups of organisms can have different rates of molecular evolution. The mean *p*-distance between the groups in our network are in the range of 1,5 to 6%, which is lower than the level suggested by Hebert *et al.* (2006). In addition, the separation of haplotype networks into unconnected networks could be sampling artefacts due to geographically widespread sampling localities and limited size of samples. The detection of intermediate haplotypes at geographically intermediate localities could reduce the amounts of mutational steps (in effect theoretical haplotypes) between unconnected networks and

thereby establishing connection between these. Moreover, Malaquias and Reid (2009) established a cut-off value between species in the genus *Bulla* at 10% uncorrected *p*-distance for COI gene and did not find the genetic breaks of the COI and 16S phylogenies to be mirrored by a phylogeny of the slower evolving nuclear gene 28S rRNA. With all of this taken into account, the suggestion by Malaquias and Reid (2008, 2009) to consider *B. occidentalis* as one single taxonomic entity seems to be valid.

A striking result was the high haplotype diversity in the COI gene (0.6667 ± 0,1409 – 1.0000 ± 0,0447), something that is both uncommon and difficult to explain. Wilson *et al.* (2009) reported similar high genetic diversity (0,6429 ± 0,184 – 0,1000 ± 0,096) for the opisthobranch *Doris kerguelenensis* from the South Atlantic/Antarctic region. Despite its direct mode of development and therefore theoretically limited dispersal capacity *D. kerguelenes* showed no shared haplotypes between major geographical regions, though within regions shared haplotypes could be found up to 450 kilometres apart (Wilson *et al.* 2009). Faster evolutionary rate in COI compared to 16S presumably has greater potential for capturing glaciation events (Wilson *et al.* 2009) and the large differentiation in the COI statistical parsimony network (Figure 7) may have been caused by this. Wilson *et al.* (2009) attributed the genetic diversity in *D. kerguelenensis* to glaciations events, where in Antarctica the ice-sheets grew over the continental shelf severely reducing the amount of available habitat and restricting survival to small pockets (Thatje 2005). Likely, with receding ice-sheets re-colonization took place followed by rapid differentiation caused by increased allele fixation due to small population sizes in refugia. Regarding *B. occidentalis* it is possible that fragmentation of populations and reduced gene-flow during Plio-Pleistocene eustasy coupled with species biological intrinsic factors could have lead to the high diversity of unique haplotypes found in this snail.

5.2. Patterns and forces of marine diversification in the TWA

5.2.1. Are present isolating mechanisms detectable for Bulla occidentalis?

The degree of genetic connectivity and longevity of larval stages in marine organisms (and thereby dispersal potential) are not always correlated, and larval longevity is therefore not necessarily a good predictor for dispersal potential (Weersing and Toonen 2009). Our results do indicate that *B. occidentalis* has a high level of connectivity throughout most of the Tropical Western Atlantic.

Clade (A) consists of a diverse assembly of sequences from vastly different localities, including the extremes of the geographical range in this study (Bermuda, Brazil and Mexico). These are separated by geographic distances of approximately 6700 km (Brazil-Mexico), 5700 km (Brazil-Bermuda) and 2700 km (Bermuda-Mexico), while the Florida Keys clade and Cuban clade lie closer to each other and deviate more genetically. There was no evidence for a clear-cut isolation-by-distance pattern in our dataset, a conclusion that is strengthened by the fact that pairwise F_{ST} values vary greatly an in a non-systematic way. Localities in the opposite range of the species distribution (e.g. Bermuda-Brazil,) have lower F_{ST} (0.36583) than localities that are geographically closer (e.g. Brazil-Guadeloupe, F_{ST} = 0.61031). Another interesting result is the fact that samples from the southern-most sampling locality at Isla Itaparica, Brazil, were not divergent compared to the rest of the sampling set. It was our expectation that this locality could be divergent due to the bifurcating nature of the South Equatorial Current System and mainly uni-directional transport of water along the Brazilian coastline as well as its large geographical distance from the remaining sampling stations. However, all Brazilian sequences fall into one well-supported sub-clade (PP = 1) with one Cuban and four Bermudan sequences, as well as being differentiated by 5–8 mutational steps in the COI haplotype network. This could indicate an ongoing diversification process, and would make an interesting hypothesis for further study at a later time.

There are several examples of studies that aim to uncover mechanisms inhibiting genetic connectivity in the TWA and it seems that different barriers apply to different animal groups (marine bivalves, Mikkelsen and Bieler 2000; *Brachidontes exustus,* Lee and Ó Foighil 2004, 2005; trochid gastropods, Diáz-Ferguson *et al.* 2010). One such hypothesis was tested, namely whether the "connectivity-hypothesis" proposed by Cowen *et al.* (2006) that recognized four regions of high connectivity (Eastern Caribbean, Western Caribbean, the Bahamas-region and the coastlines influenced by the Colombia-Panama gyre) could explain the genetic breaks observed in *B. occidentalis.* Like for trochid gastropods (Díaz-Ferguson *et al.* 2010) this hypothesis is not supported for *B. occidentalis.* Sixty-five percent of the observed variation was explained between populations within these pre-defined groups ($p < 0,05$), indicating that these regions do not realistically reflect a common pattern of surface-current mediated pattern of gene-flow.

The hypothesis of a general pattern of segregation between continental and oceanic populations due to ecological specialization (e.g. *Brachidontes exustus,* Lee and Ó Foighil 2005; *Bulla occidentalis,* Malaquias and Reid 2009) was not supported by the presented results. The phylogeny and

haplotype networks grouped oceanic and continental populations together, providing no evidence that such a mechanism is causing diversification within *B. occidentalis*. In addition, there does not seem to be a consistent pattern of higher F_{ST}-values between oceanic and continental populations pairs compared to values between continental-continental and oceanic-oceanic pairs.

5.2.2. Historical patterns and processes

The deep lineage splits within *B. occidentalis* are dated to the Late Miocene at between 11,06 – 6,11 Mya. The slightly younger node splitting groups B and C is unsupported, so we consider splits between the three main lineages (A, B and C) to be dated to the same period, several million years earlier than the final closure of the Panamanian Isthmus. However, the shoaling process that lead to the closing of the Isthmus took place over 12 million years, and it is likely that these splits are in some way related to oceanographic and geophysical changes in the region that may have caused vicariance between groups A, B and C prior to the closing of the Isthmus. There exist examples of divergences in a wide range of Trans-Isthmian geminate clades from diverse animal groups (fish, Molluscs, Crustacea and Echinodea) that do pre-date the closing of the Panamanian Isthmus (Lessios 2008).

The Strait of Florida has been described in early literature as an important barrier for dispersal of marine organisms based on large differences in fish faunas on either side of the strait (Briggs 1974). Certain properties of the Florida current, like fast flow and little mixing were put forth to explain genetic breaks in the area such as a potential barrier between Florida and the Bahamas (Briggs 1974). The Florida Keys are located in the intersection between temperate and tropical Gulf of Mexico, sub-tropical north-western Atlantic and the tropical Caribbean, and the environments on the two sides of the Florida Keys provide substantially different habitats. This has resulted in examples of genetic disjunction in species distributed on both the Atlantic and Gulf-sides of the Florida Peninsula (*Crassostrea virginica*, Reeb and Avise 1989, *Brachidontes exustus,* Lee and Ó Foighil 2004). For American oysters (*C. virginica*) this discrepancy was explained by divergence under allopatry during Pleistocene low sea-level stands that to a large degree isolated the Gulf of Mexico (see Figure 2 for illustration) from the Atlantic side of Florida (Reeb and Avise 1989). For the scorched mussel *Brachidontes*, the maintenance of genetic discontinuities was suggested to be caused by post-recruitment ecological filters, and that the origin of this genetic disjunction was slightly too old to be caused by Pleistocene transient allopatry (2.91–2.18 Ma) (Lee and Ó Foighil

2004; Lee and Ó Foighil 2005). A survey of the Florida Keys bivalve-fauna showed that the species composition of the high-salinity environment of the Florida Bay (north of the Florida Keys) has its own identity compared to other parts of the Keys (Mikkelsen and Bieler 2000), but our sampling localities are all close to the oceanic side of the Keys, so it is not clear whether the observed divergence of Florida Keys compared to the rest of the TWA can be attributed to this ecological difference. The fact that the Florida Keys form the only "geographically monophyletic" group could serve as an indication that there is a stronger driving force maintaining genetic differentiation in this lineage compared to the rest of the Caribbean.

The Yucatán current, flowing between Cuba and the Yucatán peninsula connecting the Caribbean Current and the Loop Current has a strong flow on the western side of the Yucatán strait, but a weak southern flow off the eastern tip of Cuba (Gyory [2011c]). Excess water from the Loop Current that does not enter the Florida Current constitutes this southern-bound flow, and if this flow has been sufficiently persistent through time, and strong enough to inhibit larvae from the Cuban population entering the Loop Current, then this could also have been a mechanism promoting genetic differentiation between the Cuban population and the rest of the Caribbean. The fact that the predominantly Cuban group includes specimens found in East Florida can be explained by the fact that the current pattern places East Florida downstream from Cuba increasing the probability of finding specimens from East Florida specimens in the Cuban clade. However, this picture is somewhat obscured by the fact that Cuban sequences are found in the larger group encompassing sequences from the entire region.

The origin of the biggest clade (A) that contains sequences from throughout the TWA also has its origin in the Late Miocene, but this group contains two large and well supported sub-clades that originate in Late Pliocene or Lower Pleistocene, 4,6 – 2,3 Mya. The main part of this interval pre-dates the final closure of the Panamanian Isthmus (2,8 Mya), but places it in the final stages of the Isthmus up-lift, and possibly links the lineage split to this event.

The majority of lineage splits for all the three main clades are dated to the Pleistocene, during the last 2 Ma, with the main diversification happening during the Lower to Upper Pleistocene in the last 1 Ma. This could be related to transient allopatry caused by sea level changes. Figure 2 shows that under low sea-level stands the Caribbean Sea can roughly be divided into three semi-enclosed basins, possibly with strong effects on ocean circulation patterns. If ocean circulation in the

Caribbean was reduced in strength or hindered, this could potentially reduce gene-flow throughout the Caribbean, which could lead to temporary isolation of populations – transient allopatry – allowing for genetic differentiation of isolated populations. For *D. kergelenuensis* genetic diversification was attributed to transient allopatry causing reduction in habitat size with increased selection and allele fixation, the so-called Antarctic diversity-pump (Wilson *et al.* 2009). The timing of the diversification of *B. occidentalis* lineages coincides with an increase in the magnitude of glaciations outside polar regions from approximately 1 Mya to 800 Kya as opposed to large glaciation events throughout the Quaternary as has been the common view (Ehlers and Gibbard 2007).

5.3. Demographic history

The Bayesian Skyline analysis (Figure 9) suggests a stable effective population size for *B. occidentalis* since the three main lineages split 11,06 – 6,11 Mya, suffering a small bottleneck between 1 Mya and 500 Kya followed by a large population expansion event during the last 500 Ka. This population expansion is also suggested by the negative values of Fu's Fs. The increase in Pleistocene sea level fluctuations due to glaciation would have caused an increase in periodic shifts of habitat availability.

Despite constantly changing coastal habitats during the Pleistocene it seems the causes of molluscan turnover since the closing of the Panamanian Isthmus have mainly been related to the drop in primary productivity and resulting change in the structure of food-webs (Todd *et al.* 2002; O'Dea *et al.* 2007). For bivalves, extinctions caused by the reduction in habitat availability due to receding sea-level has been suggested to be unlikely (Stanley 1986). The effect of marine regression on species extinction has been questioned by Stanley and Campbell (1981), as declining sea-level can lead to an increase in sublittoral areas, and thereby making it unlikely that marine organisms would suffer from crowding or habitat loss. However, this stands in contrast to results from Tropical Pacific islands where soft-bottom bivalves experienced local extinctions due to habitat loss during Pleistocene glaciation cycles, and were more severely affected than hard-bottom species (Paulay 1996). Climatic cooling has been suggested as a more plausible mechanism causing mass-extinctions in marine habitats than marine regression (Stanley and Campbell 1981). *B. occidentalis* is found in the tropical/temperate transitional-zone and its sister species *B. striata* inhabits temperate waters in the Eastern Atlantic (Malaquias and Reid 2008, 2009), which might suggest that

B. occidentalis has the ability to tolerate shifts in temperature regimes. The results could serve as an indication that sea-level oscillations during the Pleistocene likely presented new niche opportunities for *B. occidentalis* and that this species did not suffer from the effects of habitat loss or crowding, since receding sea-level might have created new soft-bottom habitats available for colonization.

Nevertheless, recent findings suggest that mitochondrial DNA alone has poor ability to estimate demographic parameters due to the small effective population size of the mitochondrial genome which combined with high mutation rates may obscure demographic history reconstruction (Eytan and Hellberg 2010). It seems that mitochondrial DNA is more suitable to reconstruct demographic history on short time scales. In addition, single locus-reconstructions cannot recover population history further back than to the most recent population bottleneck, meaning that a significant amount of information may have been lost in the Bayesian skyline analysis (Heled and Drummond 2008). This explains the long period of apparent stability in the effective population size observed in our analysis, and unfortunately limits our reconstruction to the last 1 Ma. A possibility for future work is to include another locus in the analysis to provide resolution for the reconstruction of the *B. occidentalis* demographic history. In addition, the assumption of neutrally evolving markers was not strictly held, something that may be a source of error in analyses of demographic and population genetic parameters.

6. CONCLUSIONS

B. occidentalis harbours intra-specific genetic diversity that is not easily explained by current factors mediating gene-flow between local populations. The results did not support the notion of oceanic/continental subdivision, correlation between geographical and genetic distance, and the integrity of regions of high connectivity. Three main lineages showing deep mitochondrial divergence were discovered, and possibly stem from vicariance during the formation of the Panamanian Isthmus in the Late Miocene. The most plausible explanation for the large present genetic variation in *B. occidentalis* seems to be transient allopatry caused by Pleistocene eustatic changes related to glaciation cycles, but the mechanisms responsible for maintaining genetic structure in three distinct groups through history are not known.

To further explore the population genetic structure in *B. occidentalis* a good strategy would be to perform comparisons at a smaller scale. Genetic break-points such as the Mona Passage and the Exuma sound will not be revealed unless the sampling design accounts for testing these hypotheses. The seasonality of spawning is also an aspect that needs to be addressed, as it is only the oceanographic conditions during larval release that will have potential to influence population connectivity, so knowledge about spawning in populations throughout the TWA is necessary for further understanding the genetic diversity of populations of *B. occidentalis*.

7. ACKNOWLEDGEMENTS

This project would not have been possible without the help of many collaborators. First of all I would like to thank my supervisors, Manuel A. E. Malaquias and Endre Willassen for being generous with their time and support. I am quite sure the allotted hours for supervision were used up after the first few months of work. Another big thank you goes to Professor Olivier Gros at the University of the French Antilles and Guyana for hospitality and assistance in the field. He made it quite enjoyable and relaxed to be an inexperienced field biologist far away from home. Thanks to Marius Kambestad for taking time during his own field work for collecting *Bulla* specimens at the Smithsonian Tropical Research Institute at Bocas del Toro in Panama.

I also want to thank my parents for both moral and financial support making it possible for me to travel to London and Guadeloupe without using all my savings and leaving room for some adventures as well as thesis work. At last I want to thank my partner Emilie who has assisted me both at home and in the field. Without you I would still be swimming in the Guadeloupean mangrove lagoons looking for *Bulla occidentalis*!

8. REFERENCES

Andrade, C.A. and Barton E.D. (2000) Eddy development and motion in the Caribbean Sea. *Journal of Geophysical Research-Oceans*, **105**, 26191-26201.

Bellwood, D.R. and Wainwright P.C. (2002) The history and biogeography of fishes on coral reefs. *Coral reef fishes* (ed. by P. F. Sale), pp. 5-32. Elsevier Science, Burlington.

Bischof, B., Mariano, A.J. and Ryan, E.H. (2003) The North Brazil Current. *Ocean Surface Currents* (http://oceancurrents.rsmas.miami.edu/atlantic/north-brazil.html). Last accessed: 22.05.2011.

Bohonak, A. J. (2002) IBD (Isolation By Distance): a program for analyses of isolation by distance. *Journal of Heredity*, **93:** 153-154.

Briggs, J.C. (1974) *Marine Zoogeography*. McGraw-Hill, New York.

Budd, A.F., Johnson, K.G. and Stemann T.A. (1996) Plio-Pleistocene turnover and extinctions in the Caribbean reef coral fauna. *Evolution and environment in Tropical America* (ed. by J. B. C Jackson, A. F. Budd and A. G. Coates), University of Chicago Press, Chicago.

Campbell Jr., K.E., Frailey, C.D. and Romero-Pittman, L. (2006) The Pan-Amazonian Ucayali Peneplain, late Neogene sedimentation in Amazonia, and the birth of the modern Amazon River system. *Palaeogeography Palaeoclimatology, Palaeoecology*, **239**: 166-219.

Chan, L.M., Brown, J.L. and Yodera, A.D. (2011) Integrating statistical genetic and geospatial methods brings new power to phylogeography. *Molecular Phylogenetics and Evolution,* **59:** 523-537.

Clement, M., Posada, D. and Crandall K. (2000) TCS: a computer program to estimate gene genealogies. *Molecular Ecology*, **9:** 1657-1660.

Coates, A.G. and Obando, J.A. (1996) The Geologic Evolution of the Central American Isthmus. *Evolution and Environment in Tropical America,* (ed. by J. B. C. Jackson, A. F. Budd and A. G. Coates). University of Chicago Press, Chicago.

Collin, R. (2003) Phylogenetic Relationships Among Calyptraeid Gastropods and Their Implications for the Biogeography of Marine Speciation. *Systematic Biology,* **52** (5): 618-640.

Cowen, R.K., Paris, B. and Srinivasan, A. (2006) Scaling of Connectivity in Marine Populations. *Science*, **311:** 522-527.

Cunha, R.L., Lopes, E.P., Reis, D.M. and Castilho, R. (2011) Genetic structure of *Brachidontes puniceus* populations in Cape Verde archipelago shows signature of expansion during the last glacial maximum. *Journal of Molluscan Studies*. **77**(2): 175-181.

Díaz-Ferguson, E., Haney, R., WARES J. and Silliman, B. (2010) Population Genetics of a Trochid Gastropod Broadens Picture of Caribbean Sea Connectivity. *Public Library of Science: One,* **5**(9): e12675. doi:10.1371/journal.pone.0012675.

Doellman, M.M., Trussel, G.C., Grahame, J.W. and Vollmer, S.V. (2011) Phylogeographic analysis reveals a deep lineage split within North Atlantic *Littorina saxatilis*. *Proceedings of the Royal Society*. doi: 10.1098/rspb.2011.0346

Drummond, A.J., Rambaut, A., Shapiro, B., and Pybus, O. G. (2005) Bayesian Coalescent Inference of Past Population Dynamics from Molecular Sequences. *Molecular Biology and Evolution,* **22:** 1185-1192.

Drummond, A.J. and Rambaut, A. (2007) BEAST: Bayesian evolutionary analysis by sampling trees. *BioMed Central: Evolutionary Biology* **7:** 214.

Drummond, A.J., Ho S.Y.W., Rawlence, N. And Rambaut, R. (2007) A rough guide to BEAST 1.4. Department of Computer Science, Auckland.

Ehlers, J. and Gibbard, P.L. (2007) The extent and chronology of Cenozoic Global Glaciation. *Quaternary International*, **164–165**, 6–20.

Excoffier, L. and Lischer, H.E.L. (2010) Arlequin suite ver 3.5: A new series of programs to perform population genetics analyses under Linux and Windows. *Molecular Ecology Resources,* **10:** 564-567.

Eytan, R.I., and Hellberg, M.E. (2010) Nuclear and mitochondrial sequence data reveal and conceal different demographic histories and population genetic processes in Caribbean reef fishes. *Evolution,* **64:** 3380-3397.

Folmer, O., Black, M., Hoeth W., Lutz, R. and Vrijenhoek, R. (1994) DNA primers for amplification of mitochondrial cytochrome c oxidase subunit I from diverse metazoan invertebrates. *Molecular Marine Biology and Biotechnology*, **3:** 294-299.

Forest, F. (2009) Calibrating the Tree of Life: fossils, molecules and evolutionary timescales. *Annals of Botany*, **104:** 789-794.

Fu, Y. (1997) Statistical Tests of Neutrality of Mutations Against Population Growth, Hitchhiking and Background Selection. *Genetics,* **147:** 915-925.

Gyory, J., Mariano, A.J. and Ryan, E.H. [2011a] The Caribbean Current, *Ocean Surface Currents* (http://oceancurrents.rsmas.miami.edu/caribbean/caribbean.html).
Last accessed: 22.05.2011.

Gyory, J., Mariano, A.J. and Ryan, E.H. [2011b] The Guiana Current, *Ocean Surface Currents* (http://oceancurrents.rsmas.miami.edu/atlantic/guiana.html). Last accessed: 22.05.2011.

Gyory, J., Mariano, A.J. and Ryan, E.H. [2011c] The Yucatan Current. *Ocean Surface Currents*. (http://oceancurrents.rsmas.miami.edu/caribbean/yucatan.html). Last accessed: 22.05.2011.

Hall, T.A. (1999) BioEdit: a user-friendly biological sequence alignment editor and analysis program for Windows 95/98/NT. *Nucleic Acids Symposium Series,* **41:** 95-98.

Hart, M.W., Keever, C.C., Dartnall, A.J. and Byrne, M. (2006) Morphological and genetic variation indicate cryptic species within Lamarck's Little Sea Star, *Parvulastra (Patiriella) exigua*. *The Biological Bulletin,* **210:** 158-167.

Hebert, P.D.N., Ratnasingham, S. and Waard, J.R.D. (2003) Barcoding animal life: cytochrome *c* oxidase subunit 1 divergences among closely related species. *Proceedings of the Royal Society,* **270:** S96–S99.

Heled, J. and Drummond, A.J. (2008) Bayesian inference of population size history from multiple loci. *BioMed Central: Evolutionary Biology* **88**(289): doi:10.1186/1471-2148-8-289.

Ho, S., and Shapiro, B. (2011) Skyline-plot methods for estimating demographic history from nucleotide sequences. *Molecular Ecology Resources*. **11**(3): 423–434.

Huddlestun, P.F. (1984) The Neogene stratigraphy of the Central Florida Panhandle. Florida State University, Tallahasseee.

Isaza, C.F.A., Sierra-Correa, P.C., Bernal-Velasquez, M., Londoño, L.M. and W. Troncoso. (2006) Global International Waters Assessment Caribbean Sea/Colombia and Venezuela, Central America and Mexico, GIWA Regional assessment 3b, 3c. United Nations Environment Programme. University of Kalmar for United Nations Environment Programme, Kalmar.

Jensen, J.L., Bohonak, A.J. and Kelley, S.T. (2005) Isolation by distance, web service v. 3.16. *BioMed Central: Genetics*, **6:**13.

Kawauchi, G.Y. and Giribet, G. (2011) On the amphi-Atlantic *Siphonaria pectinata* (Linnaeus, 1758) (Gastropoda: Heterobranchia: Siphonariidae): invader from the east or endemic? *Journal of Molluscan Studies*, **77:**196-201.

Kirkendale, L.A. and Meyer, C.P. (2004) Phylogeography of the *Patelloida profunda* group (Gastropoda: Lottidae): diversification in a dispersal-driven marine system. *Molecular ecology,* **13**(9): 2749-2762

Larkin, M.A., Blackshields, G., Brown, N.P., Chenna, R., McGettigan, P.A., McWilliam, H., Valentin, F., Wallace, I.M., Wilm, A., Lopez, R., Thompson, J.D., Gibson, T.J. and Higgins, D.G. (2007) Clustal W and Clustal X version 2.0. *Bioinformatics,* **23**: 2947-2948.

Lessios, H.A. (2008) The Great American Schism: Divergence of marine organisms after the rise of the Central American Isthmus. *The Annual Review of Ecology, Evolution, and Systematic,* **39**: 63-91.

Lee, T. and Ó Foighil, D. (2004) Hidden Floridian biodiversity: mitochondrial and nuclear gene trees reveal four cryptic species within the scorched mussel, *Brachidontes exustus*, species complex. *Molecular Ecology,* **13:** 3527–3542.

Lee, T. and Ó Foighil, D. (2005). Placing the Gloridian marine genetic disjunction into a regional evolutionary context using the scorched mussel, *Brachidontes exustus*, species complex. *Evolution,* **59**(10): 2139-2158.

Malaquias, M.A.E. and Reid, D.G. (2008) Systematic revision of the living species of Bullidae (Mollusca: Gastropoda: Cephalaspidea), with a molecular phylogenetic analysis. *Zoological Journal of the Linnean Society,* **153:** 453–543.

Malaquias, M.A.E. and Reid, D.G. (2009) Tethyan vicariance, relictualism and speciation: evidence from a global molecular phylogeny of the opistobranch genus *Bulla*. *Journal of Biogrography,* **36**: 1760-1777.

Mikkelsen, P.M. and Bieler, R. (2000) Marine bivalves of the Florida Keys: discovered biodiversity. *The Evolutionary Biology of the Bivalvia*, *Special publications* (ed. by E. M. Harper, J. D. Taylor and J. A. Crame) pp. 367-387. The Geological Society of London.

Miller, K.G., Kominz, M.A., Browning, J.V., Wright, J.D, Mountain, G.S., Katzl, M.E., Sugarman, P. J., Cramer B. S., Christie-Blick, N. And Pekar, S. F. (2005) The phanerozoic record of global sea-level change. *Science*, **310:** 1293-1298.

Miloslavich, P., Díaz, J.M., Klein, E., Alvarado, J.J., Díaz, C., Gobin, J., Escobar-Briones, E., Cruz-Motta, J.J., Weil, E., Cortés, J., Bastidas, A.C., Robertson, R., Zapata, F., Martín, A., Castillo, J., Kazandjian, A. and Ortiz, M. (2010) Marine Biodiversity in the Caribbean: Regional Estimates and Distribution Patterns. *Public Library of Science: ONE,* **5** (8): e11916.

Mueller, R.L. (2006) Evolutionary rates, divergence dates, and the performance of mitochondrial genes in Bayesian phylogenetic analysis. *Systematic B*iology, **55**(2): 289-300.

Murillo, L. and Templado, J. (1998) Spawn and development of Bulla striata (Opisthobranchia, Cephalaspidea) from the western Mediterranean. *Iberus,* **16**: 11-19.

O'Dea, A., Jackson, J.B.C., Fortunato, H., Smith, J.T., D'Croz, L., Johnson, K.G.and Todd, J.A. (2007) Environmental change preceded Caribbean extinction by 2 million years. *Proceedings of the National Academy of Science of the United States of America,* **104**(13): 5501-5506.

Palumbi, S., Martin, A., Roman, S., McMillan, W.O., Stice, L. and Grabowski, G. (2002) The Simple Fool's Guide to PCR. Department of Zoology and Kewalo Marine Laboratory, University of Hawaii, Honolulu.

Paulay, G. (1990) Effects of late Cenozoic sea-level fluctuations on the bivalve faunas of tropical oceanic islands. *Palaeobiology,* **16:** 415-434.

Reid, D.G. (2009) The genus *Echinolittorina* Habe, 1956 (Gastropoda: Littorinidae) in the western Atlantic Ocean. *Zootaxa,* **2184**: 1-103.

Roberts, C.M., Mcclean, C.J., Veron, J.E.N., Hawkins, J.P., Allen, G.R., Mcallister, D.E., Mittermeier, C.G., Schueler, F.W., Spalding, M., Wells, F., Vynne, C. And Werner, T.B. (2002) Marine biodiversity hotspots and conservation priorities for tropical reefs. *Science,* **295**, 1280-1284.

Rocha, L.A. (2003) Patterns of distribution and processes of speciation in Brazilian reef fishes. *Journal of Biogeography,* **30**: 1161-1171.

Rocha, L.A., Lindemann, K.C., Rocha, C.R. and Lessios, H.A. (2008) Historical biogeography and speciation in the reef fish genus *Haemulon* (Teleostei: Haemulidae). *Molecular Phylogenetics and Evolution,* **48:** 918-928.

Ronquist, F. and Huelsenbeck, J.P. (2003) MrBayes 3: Bayesian phylogenetic inference under mixed models. *Bioinformatics,* **19:** 1572–1574.

Rowe, E., Mariano, A.J. and Ryan E.H. [2011] The Antilles Current. *Ocean Surface Currents,* (http://oceancurrents.rsmas.miami.edu/atlantic/antilles.html). Last accessed 22.05.2011.

Saunders, J.B., Jung, P. and Biju-Duval, B. (1986) Neogene paleontology in the northern Dominican Republic. 1. Field surveys, lithology, environment, and age. *Bulletins of American Paleontology,* **89**.

Schaeffer, K. (1996) Review of data on cephalaspid reproduction, with special reference to the genus *Haminaea* (Gastropoda, Opisthobranchia). *Ophelia,* **45:** 17-37.

Spalding, M.D., Fox, H.E., Allen, G.R., Davidson, N., Ferdaña, Z.A., Finlayson, M., Halpern, B.S., Jorge, M.A., Lombana, A., Lourie, S.A., Martin, K.D., Mcmanus, E., Molnar, J., Recchia, C.A. and Robertson, J. (2007) Marine ecoregions of the world: A bioregionalization of coastal and shelf areas. *BioScience*, **57**, 573-583

Stanley, S.M. (1986) Anatomy of a Regional Mass Extinction: Plio-Pleistocene Decimation of the Western Atlantic Bivalve Fauna. *Palaios,* **1**(1): 17-36.

Stanley, S.M. and Campbell, L.D. (1981) Neogene mass extintion of Western Atlantic molluscs. *Nature,* **293**(8): 457-459.

Sunnucks, P. (2000) Efficient genetic markers for population biology. *Trends in Ecology and Evolution*, **15:** 199-203.

Tamura, K., Peterson, D., Peterson, N., Stecher, G., Nei, M., and Kumar, S. (2011) MEGA5: Molecular evolutionary genetics analysis using maximum likelihood, evolutionary distance, and maximum parsimony methods. *Molecular Biology and Evolution* (In Press).

Taylor, M.S. and Hellberg, M.E. (2006) Comparative phylogeography in a genus of coral reef fishes: biogeographic and genetic concordance in the Caribbean. *Molecular Ecology,* **15**: 695–707.

Thatje, S., Hillenbrand, C-D. and Larter, R. (2005) On the origin of Antarctic marine benthic community structure. *Trends in Ecology and Evolution,* **20**(10): 534-540.

Todd, J.A., Jackson, J.B.C., Johnson, K.G., Fortunato, H.M., Heitz, A., Alvarez, M. and Jung, P. (2002) The ecology of extinction: molluscan feeding and faunal turnover in the Caribbean Neogene. *Proceedings of the Royal Society,* **269**(1492): 571-577.

Vermeij, G.J. (2005) One-way traffic in the western Atlantic: causes and consequences of Miocene to early Pleistocene molluscan invasions in Florida and the Caribbean. *Paleobiology,* **31**(4): 624-642.

Weersing, K. and Toonen, R.J. (2009) Population genetics, larval dispersal, and connectivity in marine systems. *Marine Ecology Progress Series,* **393:** 1-12.

Weisbord, N.E. (1971) Corals from the Chipola and Jackson Bluff formations of Florida. *Geological Bulletin,* **53:** 100.

White, C., Selkoe, K.A., Watson, J., Siegel, D.A., Zacherl, D.C. and Toonen, R.J. (2010) Ocean currents help explain population genetic structure. *Proceedings of the Royal Society,* **277**: 1685-1689.

Wilson, N.G., Schrödl, M. and Halanych, K.M. (2009) Ocean barriers and glaciation: evidence for the explosive radiation of mitochondrial lineages in the Atlantic sea slug *Doris Kergulenensis* (Mollusca, Nudibranchia). *Molecular Ecology*, **18:** 965-984.

APPENDIX I – Specimen list

Country	Sampling station	Shell length (mm)	Specimen number	Museum registratin number	GenBank acc. no.	
					COI	16S
Guadeloupe	La Manche à Eau	25,39	1	Unregistered		
Guadeloupe	La Manche à Eau	26,48	2	Unregistered		
Guadeloupe	La Manche à Eau	22,4	3	Unregistered		
Guadeloupe	La Manche à Eau	21,37	4	Unregistered		
Guadeloupe	La Manche à Eau	18,33	5	Unregistered		
Guadeloupe	La Manche à Eau	20,53	6	Unregistered		
Guadeloupe	La Manche à Eau	18,43	7	Unregistered		
Guadeloupe	La Manche à Eau	20,93	8	Unregistered		
Guadeloupe	La Manche à Eau	18,2	9	Unregistered		
Guadeloupe	La Manche à Eau	17,73	10	Unregistered		
Panama	Bocas del Toro	23,09	11	Unregistered		
Panama	Bocas del Toro	17,32	12	Unregistered		
Panama	Bocas del Toro	17,18	13	Unregistered		
Panama	Bocas del Toro	16,45	14	Unregistered		
Panama	Bocas del Toro	17,64	15	Unregistered		
Panama	Bocas del Toro	19,13	16	Unregistered		
Panama	Bocas del Toro	24,58	17	Unregistered		
Panama	Bocas del Toro	12,95	18	Unregistered		
Panama	Bocas del Toro	16,69	19	Unregistered		
Panama	Bocas del Toro	13,72	20	Unregistered		
Bermuda	Tom Moore's Pond	16,82	23	ZMBN83037.3		
Bermuda	Tom Moore's Pond	15,77	24	ZMBN83037.4		
Bermuda	Tom Moore's Pond	14,08	25	ZMBN83037.5		
Bermuda	Tom Moore's Pond	14,82	26	ZMBN83037.6		
Bermuda	Tom Moore's Pond	15,34	27	ZMBN83037.7		
Bermuda	Tom Moore's Pond	14,12	28	ZMBN83037.8		
Bermuda	Tom Moore's Pond	15,57	29	ZMBN83037.9		
Bermuda	Tom Moore's Pond	13,31	30	ZMBN83037.10		
Venezuela	Laguna el Ocho, Higuerote	13,94	31	ZMBN84901.1		
Venezuela	Laguna el Ocho, Higuerote	16,96	32	ZMBN84901.2		
Venezuela	Laguna el Ocho, Higuerote	14,86	34	ZMBN84901.4		
Venezuela	Laguna el Ocho, Higuerote	14,16	35	ZMBN84901.5		
Venezuela	Laguna el Ocho, Higuerote	17,01	36	ZMBN84901.6		

Venezuela	Laguna el Ocho, Higuerote	16,1	37	ZMBN84901.7		
Venezuela	Laguna el Ocho, Higuerote	15,25	38	ZMBN84901.8		
Venezuela	Laguna el Ocho, Higuerote	15,73	39	ZMBN84901.9		
Venezuela	Laguna el Ocho, Higuerote	15,49	40	ZMBN84901.10		
Venezuela	Los Mogotes, Isla Tortuga	15,15	41	ZMBN84902.1		
Venezuela	Los Mogotes, Isla Tortuga	14,84	42	ZMBN84902.2		
Venezuela	Los Mogotes, Isla Tortuga	14,79	43	ZMBN84902.3		
Venezuela	Los Mogotes, Isla Tortuga	13,56	44	ZMBN84902.4		
Venezuela	Los Mogotes, Isla Tortuga	15,99	45	ZMBN84902.5		
Venezuela	Los Mogotes, Isla Tortuga	14,5	46	ZMBN84902.6		
Venezuela	Los Mogotes, Isla Tortuga	13,86	47	ZMBN84902.7		
Venezuela	Los Mogotes, Isla Tortuga	13,57	48	ZMBN84902.8		
Venezuela	Los Mogotes, Isla Tortuga	13,02	49	ZMBN84902.9		
Venezuela	Los Mogotes, Isla Tortuga	12,31	50	ZMBN84902.10		
Brazil	Itaparica Island	27,29	51	ZMBN86412.1		
East Florida	St. Lucie Inlet	16,92	61	UF303042.1		
East Florida	St. Lucie Inlet	16,68	62	UF303042.2		
East Florida	St. Lucie Inlet	17,09	63	UF303042.3		
East Florida	St. Lucie Inlet	13,54	64	UF303042.4		
East Florida	St. Lucie Inlet	14,19	65	UF303042.5		
East Florida	St. Lucie Inlet	14,6	66	UF303042.6		
East Florida	St. Lucie Inlet	16,9	67	UF303042.7		
East Florida	St. Lucie Inlet	13,53	69	UF303042.9		
East Florida	St. Lucie Inlet	16,93	70	UF303042.10		
Cuba	Bahia de Cienfuegos	20,8	71	Unregistered		
Cuba	Bahia de Cienfuegos	19,87	74	Unregistered		
Mexico	Laguna de Chelem	23,02	81	BMNH20070095		
Mexico	Laguna de Chelem	20,31	82	BMNH20070096		
Mexico	Laguna de Chelem	21,07	83	BMNH20070097		
Mexico	Laguna de Chelem	23,35	84	BMNH20070098.1		
Mexico	Laguna de Chelem	23,5	85	BMNH20070098.2		
Mexico	Laguna de Chelem	23,19	86	BMNH20070098.3		
Mexico	Laguna de Chelem	26,22	87	BMNH20070098.4		
Mexico	Laguna de Chelem	23,76	89	BMNH20070098.6		
Florida Keys	Pine Channel	14,06	98	BMNH20070602.1		
Florida Keys	Pine Channel	12,68	99	BMNH20070602.2		
Florida Keys	Pine Channel	10,47	100	BMNH20070602.3		
Florida Keys	Pigeon Key	-	102	BMNH20030776	DQ986544	DQ986605
Florida Keys	Long key	-	103	BMNH20030779.1	DQ986543	DQ986603
Florida Keys	Long key	-	104	BMNH20030779.2	DQ974657	DQ986604

Cuba	Playa Giron	9,68	111	ZMBN86412.2		
Cuba	Playa Giron	10,22	113	ZMBN86412.4		
Cuba	Playa Giron	9,24	115	ZMBN86412.6		
Cuba	Playa Giron	19,46	116	ZMBN86412.7		
Cuba	Playa Giron	10,36	118	ZMBN86412.9		
Cuba	Playa Giron	9,52	119	ZMBN86412.10		
Brazil	Isla Itaparica	24,81	125	Unregistered		
Brazil	Isla Itaparica	29,65	128	Unregistered		
Brazil	Isla Itaparica	26,6	129	Unregistered		
Brazil	Isla Itaparica	25,03	131	ZMBN86412.2		
Brazil	Isla Itaparica	27,36	133	ZMBN86412.4		
Brazil	Isla Itaparica	25,06	136	ZMBN86412.7		
Brazil	Isla Itaparica	24,1	139	ZMBN86412.10		
Cuba	Guanahacabibes	-	140	BMNH20060125	DQ986538	DQ986598
Cuba	Cabo de Santo Antonio	-	141	BMNH20050351.1	DQ986539	DQ986599
Cuba	Cabo de Santo Antonio	-	142	BMNH20050351.2	DQ986540	DQ986600
Cuba	Cabo de Santo Antonio	-	143	BMNH20050351.3	DQ986541	DQ986601
Cuba	Cabo de Santo Antonio	-	144	BMNH20050351.4	DQ986542	DQ986602
Brazil	Recife	-	145	BMNH20030341.1	DQ986545	DQ986606
East Florida	Saint Lucie Inlet	-	148	UF303042.1	DQ986549	DQ986610
East Florida	Saint Lucie Inlet	-	149	UF303042.3	DQ986551	DQ986611
East Florida	Saint Lucie Inlet	-	150	UF303042.4	DQ986552	DQ986612
East Florida	Saint Lucie Inlet	-	152	UF303042.6	DQ986554	DQ986614
East Florida	Saint Lucie Inlet	-	153	UF303042.7	DQ986555	DQ986615
Panama	Bocas del Toro	-	154	BMNH20060118	DQ974658	DQ986616

APPENDIX II – Nucleotide substitution model parameters

COI

Model	HKY+G+I
Akaike Information Criterion	4296,3841428608
Proportion of invariant sites (I)	0,5357819676
Gamma shape parameter (G)	0,7897452939
Transition/Transversion-bias (R)	13,9365336378
Freq A	0,2255688727
Freq T	0,3611603266
Freq C	0,2017022755
Freq G	0,2115685253

Substitution matrix

From\To	A	T	C	G
A	-	0,0118645147	0,006626142	0,1976680069
T	0,007410186	-	0,1884499915	0,0069502592
C	0,007410186	0,3374312972	-	0,0069502592
G	0,2107485006	0,0118645147	0,006626142	-

16S

Model	GTR+G
Akaike Information Criterion	1868,5725129812
Proportion of invariant sites (I)	N/A
Gamma shape parameter (G)	0,05
Transition/Transversion-bias (R)	2,2768086373
Freq A	0,2878787879
Freq T	0,3039461977
Freq C	0,1598628775
Freq G	0,2483121369

Substitution matrix

From\To	A	T	C	G
A	-	0,1135684234	0,0008068587	0,1285489704
T	0,1075648925	-	0,1568706487	0
C	0,0014529796	0,2982570935	-	0,0267051423
G	0,1490322714	0	0,0171927194	-

APPENDIX III – Isolation-by-distance geographical distances

Straight distances (km)

Tom Moore's pond	1	-										
St. Lucie inlet	2	1600	-									
Long Key	3	1780	270	-								
Pine Channel	4	1840	300	58	-							
Cabo de San Antonio	5	2310	760	530	480	-						
Playa Girôn	6	1970	570	305	290	405	-					
Laguna de Chelem	7	2760	1170	990	930	495	900	-				
Bocas del Toro	8	3120	1980	1720	1700	1420	1410	1550	-			
Higuerote	9	2420	2390	2250	2290	2410	2080	2830	1805	-		
Isla Tortuga	10	2370	2370	2240	2280	2410	2080	2840	1860	90	-	
La Manche á Eau	11	1800	2260	2215	2260	2530	2140	3010	2370	810	716	-
Isla Itaparica	12	5710	6300	6190	6220	6340	6020	6730	5390	3940	3950	4085
		1	2	3	4	5	6	7	8	9	10	11	12
		Tom Moore's pond	St. Lucie inlet	Long Key	Pine Channel	Cabo de San Antonio	Playa Girôn	Laguna de Chelem	Bocas del Toro	Higuerote	Isla Tortuga	La Manche á Eau	Isla Itaparica

Oceanographic distances (km)

Tom Moore's pond	1	-										
St. Lucie inlet	2	1600	-									
Long Key	3	1880	310	-								
Pine Channel	4	1950	380	70	-							
Cabo de San Antonio	5	2440	865	550	490	-						
Playa Girôn	6	2990	1410	1070	1020	460	-					
Laguna de Chelem	7	2910	1350	995	940	510	990	-				
Bocas del Toro	8	3980	2390	2070	2010	1430	1415	1870	-			
Higuerote	9	5160	3500	3180	3130	2480	2230	2970	1970	-		
Isla Tortuga	10	5160	3500	3180	3130	2480	2230	2970	1970	90	-	
La Manche á Eau	11	1800	2295	3450	3390	2780	2390	3180	2370	810	720	-
Isla Itaparica	12	6360	8500	8180	8120	7530	7290	7920	6960	5100	5030	5870
		1	2	3	4	5	6	7	8	9	10	11	12
		Tom Moore's pond	St. Lucie inlet	Long Key	Pine Channel	Cabo de San Antonio	Playa Girôn	Laguna de Chelem	Bocas del Toro	Higuerote	Isla Tortuga	La Manche á Eau	Isla Itaparica

APPENDIX IV – COI and 16S gene chronograms

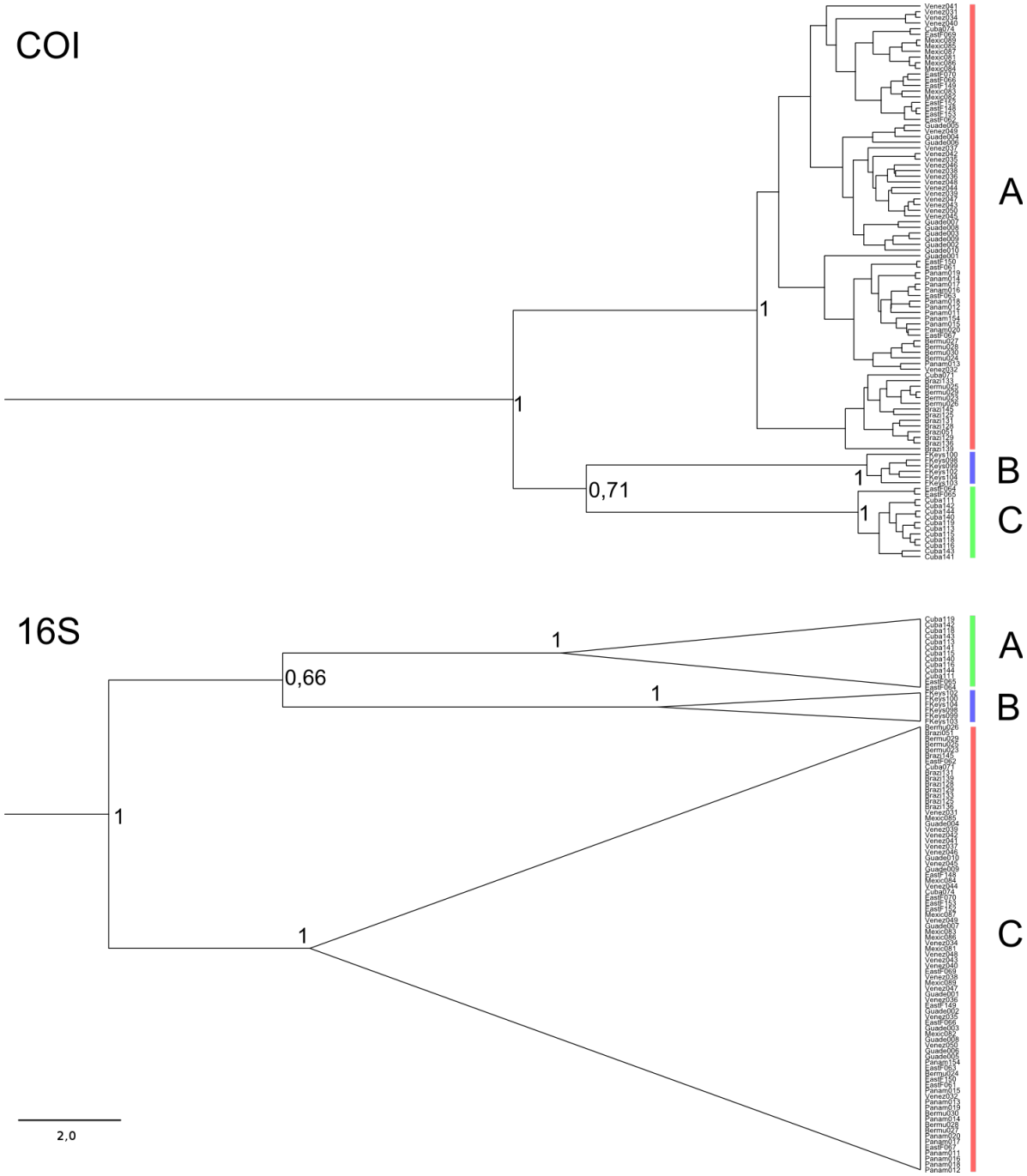

COI and 16S gene chronograms show the same basic topology with the same three well-supported main groups, with an unsupported node between groups A and B. Posterior probabilities shown above branches, and scale reported in million years. There was a problem with the 16S run causing it to struggle to reach convergence, and producing problems in the branching pattern within clade C. However, the two trees are included to show that the three deep lineages are retrieved from both genes when analysed alone.